

THE
IIOAB
JOURNAL

VOLUME 1 : NO 4 : DECEMBER 2010 : ISSN 0976-3104



Institute of Integrative Omics and
Applied Biotechnology Journal

Dear Esteemed Readers, Authors, and Colleagues,

I hope this letter finds you in good health and high spirits. It is my distinct pleasure to address you as the Editor-in-Chief of Integrative Omics and Applied Biotechnology (IIOAB) Journal, a multidisciplinary scientific journal that has always placed a profound emphasis on nurturing the involvement of young scientists and championing the significance of an interdisciplinary approach.

At Integrative Omics and Applied Biotechnology (IIOAB) Journal, we firmly believe in the transformative power of science and innovation, and we recognize that it is the vigor and enthusiasm of young minds that often drive the most groundbreaking discoveries. We actively encourage students, early-career researchers, and scientists to submit their work and engage in meaningful discourse within the pages of our journal. We take pride in providing a platform for these emerging researchers to share their novel ideas and findings with the broader scientific community.

In today's rapidly evolving scientific landscape, it is increasingly evident that the challenges we face require a collaborative and interdisciplinary approach. The most complex problems demand a diverse set of perspectives and expertise. Integrative Omics and Applied Biotechnology (IIOAB) Journal has consistently promoted and celebrated this multidisciplinary ethos. We believe that by crossing traditional disciplinary boundaries, we can unlock new avenues for discovery, innovation, and progress. This philosophy has been at the heart of our journal's mission, and we remain dedicated to publishing research that exemplifies the power of interdisciplinary collaboration.

Our journal continues to serve as a hub for knowledge exchange, providing a platform for researchers from various fields to come together and share their insights, experiences, and research outcomes. The collaborative spirit within our community is truly inspiring, and I am immensely proud of the role that IIOAB journal plays in fostering such partnerships.

As we move forward, I encourage each and every one of you to continue supporting our mission. Whether you are a seasoned researcher, a young scientist embarking on your career, or a reader with a thirst for knowledge, your involvement in our journal is invaluable. By working together and embracing interdisciplinary perspectives, we can address the most pressing challenges facing humanity, from climate change and public health to technological advancements and social issues.

I would like to extend my gratitude to our authors, reviewers, editorial board members, and readers for their unwavering support. Your dedication is what makes IIOAB Journal the thriving scientific community it is today. Together, we will continue to explore the frontiers of knowledge and pioneer new approaches to solving the world's most complex problems.

Thank you for being a part of our journey, and for your commitment to advancing science through the pages of IIOAB Journal.



Yours sincerely,

Vasco Azevedo

Vasco Azevedo, Editor-in-Chief
Integrative Omics and Applied Biotechnology
(IIOAB) Journal



Prof. Vasco Azevedo
Federal University of Minas Gerais
Brazil

Editor-in-Chief

Integrative Omics and Applied Biotechnology (IIOAB) Journal Editorial Board:



Nina Yiannakopoulou
Technological Educational Institute of Athens
Greece



Jyoti Mandlik
Bharati Vidyapeeth University
India



Rajneesh K. Gaur
Department of Biotechnology, Ministry of Science and Technology
India



Swarnalatha P
VIT University
India



Vinay Aroskar
Sterling Biotech Limited
Mumbai, India



Sanjay Kumar Gupta
Indian Institute of Technology
New Delhi, India



Arun Kumar Sangaiah
VIT University
Vellore, India



Sumathi Suresh
Indian Institute of Technology
Bombay, India



Bui Huy Khoi
Industrial University of Ho Chi Minh City
Vietnam



Tetsuji Yamada
Rutgers University
New Jersey, USA



Moustafa Mohamed Sabry Bakry
Plant Protection Research Institute
Giza, Egypt



Rohan Rajapakse
University of Ruhuna
Sri Lanka



Atun RoyChoudhury
Ramky Advanced Centre for Environmental Research
India



N. Arun Kumar
SASTRA University
Thanjavur, India



Bui Phu Nam Anh
Ho Chi Minh Open University
Vietnam



Steven Fernandes
Sahyadri College of Engineering & Management
India

ARTICLE TYPE: GENE DISCOVERY

CLONING AND CHARACTERISATION OF ALKALI MYOSIN LIGHT CHAIN GENE (MLC-3) OF CATTLE FILARIAL PARASITE SETARIA DIGITATA

Arumugam Muruganathan, Eric Hamilton Karunanayake*, Kamani Hemamala Tennekoon

Institute of Biochemistry, Molecular Biology and Biotechnology, University of Colombo, 90, Cumaratunga Munidasa Mawatha, Colombo 03, SRI LANKA

Received on: 19th-July-2010; Revised on: 28th-September-2010; Accepted on: 14th-Oct-2010; Published on: 1st-Nov-2010.

*Corresponding author: Email: erick@ibmbb.cmb.ac.lk Tel: +94-112552528; Fax: +94-112553683

ABSTRACT

Lymphatic filariasis is a tropical disease caused by filarial parasites including Wuchereria bancrofti. Although bancroftian filariasis causes severe disabling and debilitating clinical conditions in human, very little is known about the molecular biology of the parasite. The paucity of parasitic material is the main reason for this lack of knowledge. Setaria digitata is a cattle filarial parasite, closely resembling W. bancrofti in many aspects. Therefore it can be used as a model organism to study W. bancrofti. In the present study, the genomic library of S. digitata adult parasites was constructed and probed with a ³²P labeled partial mRNA sequence PCR amplified from a previously isolated cDNA clone containing a 661 bp mRNA transcript of S. digitata alkali myosin light chain gene. Isolated positive clones were sequenced and edited by using bioinformatics tools. Though the 5' flanking region did not reveal any consensus TATA box sequences, a potential CAAT box like sequence, CCAAT and seven possible transcription factor elements were identified. The entire gene had four exons encoding 149 amino acids interrupted by three introns of varying lengths of 87, 295 and 69 bp respectively. Sequences around the splice junctions were fairly conserved and agreed with the general GT-AG splicing rule. The 3' flanking region consists of three putative polyadenylation signals with the sequence AATAAA. The gene was AT rich with a GC content of 35%. Southern hybridisation studies suggested that this gene is likely to be a single-copy gene. Homology search of amino acid sequences showed more than 80% similarity with Caenorhabditis species and 40-50% with other vertebrate and invertebrate myosin light chains. Analysis of the amino acid sequence with the NCBI conserved domain database for interactive domain family identified the protein as a member of calcium binding protein family as it comprised of two highly conserved EF hand motifs, and may suggest a possible function in Ca²⁺ binding.

Keywords: Myosin; Setaria digitata; Genomic library; Filarial parasite; EF hand

[1] INTRODUCTION

Setaria digitata is a common filarial nematode that parasitises in the peritoneal cavity of cattle and buffalo. Though the infections in natural host are usually non-pathogenic, accidental transmission of the infective larva to aberrant hosts such as sheep and goat by mosquitoes results in cerebrospinal nematodiasis [1]. In Sri Lanka cerebrospinal nematodiasis is a major setback in goat and sheep husbandry that leads to severe economic losses especially in the dry zone of the country [2]. One of the constraints in the treatment and eradication of filariasis is that little is known about the biology of these parasites at molecular level. Though a number of protein coding genes have been characterised from other parasitic nematodes

only a few of these are from filariids and only two from *S. digitata* [3].

Lymphatic filariasis, a disabling and disfiguring tropical disease is caused by the tissue dwelling filaroids species *Wuchereria bancrofti*, *Brugia malayi* and *B. timori*. Around 120 million people living in 83 countries have already been infected and 1.307 billion people (20% of the population) are at risk of acquiring the infection in the tropics including Sri Lanka and in some sub tropical areas worldwide [4, 5]. Approximately 90% of the cases are caused by *W. bancrofti* and the majority of the remainder by *B. malayi* [6].

Human filariasis in Sri Lanka is caused by *W. bancrofti*, but the parasite material is not easy to obtain. Adult parasites that live

in lymphatics are not accessible and nocturnally periodic microfilariae cannot be cultured in the laboratory. Presence of adult *S. digitata* worms in the peritoneal cavity of cattle provides readily available material for investigations. It closely resembles the *W. bancrofti* not only in morphological and histological aspects [7] but also in antigenic properties [8]. *S. digitata* thus become a useful model organism to study the molecular biology of *W. bancrofti*.

Myosin is an ubiquitous actin based motor molecule present in both muscle and non-muscle cells of eukaryotes. The conventional myosin of vertebrate skeletal muscle is a hexamer composed of two heavy chains and two pairs of light chains. Based on the solubility, myosin light chains (MLCs) can be further divided into to alkali and regulatory myosin light chains. The former class can be dissociated from the myosin heavy chain in high pH conditions whereas the other one can be extracted with 5-5'-dithiobis (2-nitrobenzoic acid) (DTNB). The alkali myosin light chain of skeletal muscle is further divided into two types MLC1 and MLC3. These two types differ from each other due to the divergence of the amino acid sequences in their amino terminus and they are identical in sequence over their C-terminal [9]. Myosin like proteins have been identified as potential antigens from various filarial parasites [10 – 13]. In our previous studies two antigens of *S. digitata* with molecular weights of 52 and 130 kD showed strong cross reactivity with the serum of *W. bancrofti* infected individuals [14]. When a cDNA library of adult *S. digitata* was immunoscreened with the sera of *W. bancrofti* infected individuals, a clone designated PCSA1 showed very strong reactivity [15]. Bioinformatics analysis confirmed that the mRNA sequence coded for a protein 83% homologous with the alkali (essential) myosin light chain gene of the free living nematode *Caenorhabditis* species. It was also homologous with a 343 bp partial mRNA of the filarial parasite *Brugia malayi* [Genbank: XM_001894833] encoding a hypothetical protein. Similar nucleotide sequences have not been reported for other parasitic nematode. Thus by considering the veterinary importance, immunogenic potential and the lack of information about this gene in filarial nematodes, the objective of the present investigation was to clone and characterize the whole gene at the molecular level.

[II] MATERIALS AND METHODS

2.1. Parasites

Adult *S. digitata* worms were collected from the peritoneal cavity of cattle slaughtered at Kandy abattoir, Sri Lanka. The motile worms were immediately transported to the laboratory and repeatedly washed with phosphate buffered saline to avoid contamination by any cattle tissue or blood and stored at -70°C until use.

2.2. DNA Extraction

Genomic DNA of adult *S. digitata* was extracted, ethanol precipitated and reconstituted in TE (pH 8) buffer by the method described previously [16] and stored at -20°C until use.

2.3. Construction of genomic Library

Genomic DNA of *S. digitata* was partially digested with the restriction enzyme *Sau3A1* to yield fragments of 5 to 12 kb in length. The fragments were separated by electrophoresis on low melting agarose and suitable fragments (5 to 12 kb) were eluted using illustra GFX PCR DNA and gel band purification kit (Catalogue no. 28-9034-70, GE Healthcare Biosciences, USA).

Genomic library was constructed by using the ZAP Express Predigested Gigapack Cloning Kit (Catalog no. 239615, Stratagene, Switzerland). Briefly, the purified genomic fragments were ligated to Zap express vector pre-digested with *BamH1* and dephosphorylated. Ligated products were packaged in vitro by using the Gigapack Gold111 packaging extract. The primary library was amplified by using the *E. coli* strain XL1Blue MRF (Catalog no. 200301, Stratagene, Switzerland) and stored at 4°C in 0.7% chloroform.

2.4. Preparation of the probe

A previously isolated cDNA clone of *S. digitata* [15] carrying a length of 661bp mRNA transcript consisting of the 450 bp full open reading frame of myosin light chain gene was used to generate the PCR primers (sense primer 5'-ACTATACGACGAGGAATTGG-3' ; anti-sense primer 5'-CGAAAGAAAGCAGAAGGAGTATG-3') to amplify 510 bp middle region of the insert. The amplified PCR product was purified from low melting agarose gel and radio labeled with ³²P (Catalog no. NEG013H, Perkin Elmer, USA) by random priming method [17].

2.5 Screening the genomic library

A total of 20 plates (132 mm) each containing approximately 2000 plaque forming units were plaque lifted and screened by in situ plaque hybridization on duplicate colony/plaque screen hybridization membrane (Catalogue no. NEF978Y, Perkin Elmer, USA) as previously described with few modifications [18]. Briefly the filters were prehybridized for two hours at 65°C in the 100 µlcm⁻² prehybridization solution of 20×SSC (1×SSC= 0.15 M NaCl, 0.015 M trisodium citrate), 5× Denhardt's and 100 µg ml⁻¹ of denatured salmon sperm DNA. After discarding the prehybridization solution, hybridization was performed overnight at 65°C with the hybridization solution (50 µlcm⁻²). This contained 0.5% SDS and ³²P labeled probe in addition to the constituents of the prehybridization solution. Post hybridization washing was carried out at 65°C with the preheated (65°C) 2×SSC and 0.5% SDS for one hour with three changes. Autoradiography was performed by exposing the filters to Amersham Hyperfilm MP (Catalogue no. 28-9068-45, GE Healthcare Biosciences, USA) at -70°C with intensifying screen. Secondary and tertiary screening was performed as described above and the well isolated positive plaques were picked and stored at 4°C with 0.7% chloroform.

2.6. Southern blot analysis

Aliquots of *S. digitata* genomic DNA (3 µg) was cleaved individually with five fold excess of four different restriction enzymes *EcoR1*, *BamH1*, *Hind111* and *Sal1*. DNA fragments were separated by electrophoresis on an agarose gel with a 1kb ladder. A photograph was taken after placing a fluorescent gel ruler alongside the ladder lane and then visualizing the bands under UV. Separated fragments were partially depurinated by incubating in 0.25 M HCl (15 min at room temperature) and transferred to nitrocellulose membrane [17]. The blotted membrane was hybridized with the same probe used to screen the genomic library

as described earlier. The distance of migrated ladder bands were measured by comparing with the ruler scale using the above photograph and the locations were depicted schematically in the autoradiogram.

2.7. In-vivo excising and Restriction analysis

Isolated clones were in-vivo excised by using the Bacterial strains XL1Blue MRF (Catalog no. 200301, Stratagene, Switzerland), XL0LR (Catalog no. 200304, Stratagene, Switzerland) and the ExAssist Interference-Resistant Helper Phage (Catalog no. 200253, Stratagene, Switzerland) according to the single clone excision procedure recommended by the manufacturer to obtain the Kanamycine resistant PBK-CMV phagemid form. Candidate clones were screened for the insert size by restriction digestion with two enzymes, *Xba*1 and *Sac*1.

2.8. Sequencing

One clone designated pSMC-3 carrying an insert size of ~2kb was fully sequenced using MegaBACE 1000 automated sequencing system (GE Healthcare Biosciences, USA) using universal T3, T7 primers and the gaps were filled with synthetic oligonucleotides. Resulted sequences were deposited in the GenBank data bank at the National Center for Biotechnology Information (NCBI) under the accession number of GQ227356.1.

2.9. Bioinformatic analysis

The open reading frame (ORF) of the MLC-3 mRNA was predicted using the ORF finder program at NCBI by submitting the complete cDNA sequence as query sequence [19]. Amino acid sequences of *Brugia malayi* (Hypothetical protein), *C. briggsae* CBR-MLC-3, *C. elegans* mlc-3, *C. brenneri* mlc-3 were acquired by executing an interactive protein-protein BLAST at NCBI [20] using the amino acid sequence of *S. digitata* alkali myosin light chain as the query sequence. Multiple alignment of nucleotide sequences was carried out using ClustalW of the BioEdit software program. Analysis of amino acid sequence for interactive domain family was done with the NCBI conserved domain database [21]. PSORT II program was used to predict the sub cellular localization of the characterized protein from the amino acid sequence [22]. WWWSIGNAL SCAN transcription factor database, which predict the common eukaryotic transcriptional elements was used to analyse the sequence of the 5' UFR [23].

[III] RESULTS AND DISCUSSION

The genomic clone designated pSMC-3 isolated from the genomic library of *S. digitata* contained the complete gene including the 5' and 3' flanking region of which 580 bp and 541 bp were sequenced respectively. Comparative analysis of the genomic and cDNA sequences showed that the 450 bp long open reading frame was interrupted by three introns in positions 76-3, 98-3 and 138-1. The introns positions were numbered by considering the initiator methionine as codon 1 and the codon split after the first or second nucleotides were given the phase number -1 and -2 respectively, while -3 indicates that the intron

directly follows the codon. As observed from many other parasitic and non-parasitic nematodes [18, 24, 25], the introns were relatively short with varying lengths of 87 bp, 295 bp and 69 bp respectively [Figure-1].

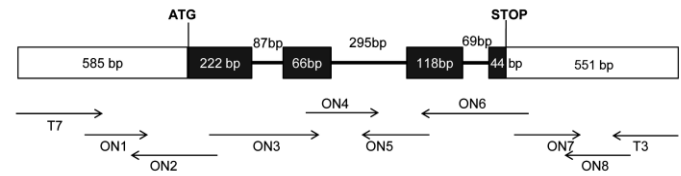


Fig. 1. Schematic representation of the alkali myosin light chain gene of *S. digitata*: Boxed regions are exons. Protein coding portion of the genes are shaded. 5' and 3' untranslated regions are open. Arrows indicate sequencing strategy used. ON=synthetic oligonucleotides.

Alignment of sequence around the 5' (donor) and 3' (acceptor) splice junctions of *S. digitata* alkali myosin light chain gene with the consensus sequences for eukaryotes [26] identified that the sequences around the splice junctions are fairly conserved [Figure-2] and agreed with the general GT-AG splicing rule of the eukaryotes and also with those of parasitic nematodes [24]. Moreover from this alignment it was possible to develop a consensus for the sequence around the splice sites of *S. digitata*. This consensus would be useful to identify exon-intron junctions of other genes that may be cloned from this parasite in the future.

Analysis of the 5' flanking region did not reveal any consensus TATA box sequences but, the potential CAAT box like sequence, CCAAT was identified at nucleotide position -449. Though there is no data available on the 5' flanking region of similar myosin light chain gene of other filarial nematodes to compare possible common regulatory elements, analysis of the sequence with the WWWSIGNAL SCAN transcription factor database hypothetically identified seven possible regulatory elements. Details of the identified elements are summarized in Table-1. It has been reported that there are some myosin light chain genes using atypical sequences instead of consensus TATA sequence [27].

The analysis of the 3' UTR revealed three polyadenylation signals 143 bp, 168 bp and 410 bp downstream from the stop codon respectively [Figure-3]. Comparative analysis of the cDNA clone revealed that the first polyadenylation signal located 143 bp downstream from the stop codon was utilized. The molar ratio of A: T and G: C generally known as GC content is an important parameter of genome in the analysis of phylogenetic relationship. Filariids are reported to have some of the most AT rich genome [28]. The G+C content of the entire gene including the 3' and 5' UTR was 35% while the coding region had a G+C content of 44%. The introns were A+T rich (69%) while the 5' and 3' UTR have an AT content of 68%.

| Regulatory element | Signal Sequence | Location | Number of copies |
|--------------------|-----------------|----------------|------------------|
| CBF | ATTGG | -454, -451 | 2 |
| CDF | ATTGG | -454, -451 | 2 |
| GATA-1 | WGATAMS | -543 | 1 |
| H1_conserved_US | AAACACA | -417 | 1 |
| H2A_conserved_U | YCATTG | -321 | 1 |
| Myb | YAACKG | -461,-374,-299 | 3 |
| PEA3 | AGGAAR | -245 | 1 |

Table: 1. Regulatory elements in the 5' flanking region of the alkali myosin light chain gene of *S. digitata* identified by the WWWSIGNAL SCAN transcription factor database.

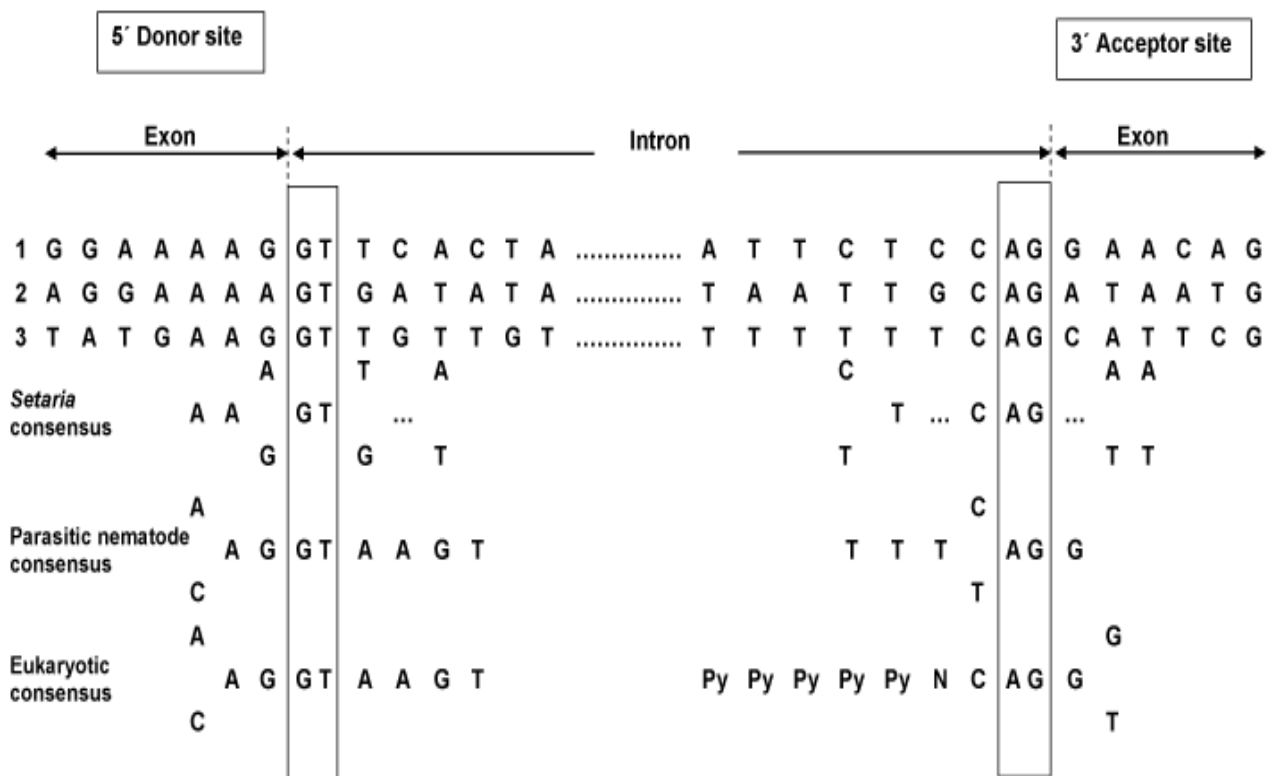


Fig: 2. Alignment of the sequence around 5' and 3' splice junctions. Comparison of sequence around 5' and 3' splice junctions of *S. digitata* alkali myosin light chain gene with consensus sequences for parasitic nematodes and Eukaryotes. Py = pyrimidine

```

1  GAATATAATTTTCGATCATACTGATTATAACCGATTTATTCTGATAACAGCTCTACGAGAACAAAATTCT
71  GTTACTGGTTGCAATTATTCGTCCTTCCGGTCGAATTCGAAAATTCAAACCTTAACAGTTGTCCAATTTGGC
141 TGAAAAAAGAATTCTTGTTCCTTAAGTGTGTTGCATACGTTTTTCCAGTCTGTTCAAGTCCCTCTAA
211 GCAACTGTTCATGCTAGTAGTCTTAATTCCATCTTCTCCTCAGTAATCATCTAGTCCCTATCAGACCTTT
281 CAGCAATAACTGCTCTCAGCATCTTACAATCATCAGCTACAAGAAGCAATTAATTAGAGAGGAAAAGAA
351 CAGGGAATGAGACAGCAGTAAATAAGTTAGCAGAGAAAATGAGAAAAAGTGTTCAGAAAAAGTGACA
421 AATTATCAGAGTAAAAAATATTTATAAATTAGAAAAGTACTGATGAAGGAATTATTCTGATGCATCTT
491 TGCTATAAGGAATCGGATGCAACATTTGGATGACCCCTAGTTTCGGGTCATCTACCATACCTAGAAAGAGA
561 TGTAGAGAGGTCGGTTAAGTGACAAATGTTAATTGCAGAGCTGAAAGAAATATTCTTACTATACGACGAG
      M L I A E L K E I F L L Y D E
631 GAATTGGATGGGAAGATAGATGGCACTCAAATTGGCGATGTTGTTTCGAGCTGCTGGACTGAAACCCACCA
      E L D G K I D G T Q I G D V V R A A G L K P T
701 ATGCAATGGTAGTTAAGGCAAGTGAAGTGAATACAAACGAAAAGGTGAAAACGTTTGACATTCGAAGA
      N A M V V K A S G S E Y K R K G E K R L T F E
771 ATGGATGCCAATTTATGAGCAGCTCAGCAAGGAAAAGgttcactatttctcttcattttgcatcgattat
      E W M P I Y E Q L S K E K
841 gtcttgattggttattatcgaagaacggaattacatttgacgtttatttctccagAACAGGGAACGTTTC
      E Q G T F
911 AGGATTTTCGTTGAGGGATTGAAAGTTTTTCGACAAAGAGGAGTCAGGAAAAGtgatatataatgtctat
      Q D F V E G L K V F D K E E S G K
981 tttgtatactatTTTTTTTTtaatctctgtttgttcaaatttcaaacaatcctggattagattccttaggatg

1051 ttacggagaagagaaaaatcaatcacattttttgggttcggatcacaataatggactttttatactttta

1121 taattcatgtctcacatttacattctttcattgctaacaacgattcaatcgacacagtcattcatgta

1191 aaaaatcaagcaattaattaatggttgcgtacagataggttaattagtaatgatatgcttaattgcagATAA
      I
1261 TGGCTGCAGAATTAAGGCATGTGTTGATGGCTCTAGGAGAGCGTCTGTCAGCTGAAGAAGCAGATGAAAT
      M A A E L R H V L M A L G E R L S A E E A D E
1331 AATGAAAGGATGTGAAGATGCGGAAGGCATGGTTTCCCTATGAAGgttggttggtgcatcagttccatagaa
      I M K G C E D A E G M V S Y E
1401 gcaactgatcattcagaattcttgttccataccttttttttcagCATTCGTCAGAAGGTGCTAGCTGGAC
      A F V K K V L A G
1471 CGTTTCCGGACGATTGAGTCGGTTCAGTGCTCAACAATATACTTCAGTTCAGACCATCCACACTACGAG
      P F P D D
1541 AAAAAACACTCATACTCCTTCTGCTTTCTTTTCGAAATGTTCAACTAATTTCAAATTAATTCCTTCA
1611 AATCTTATTTCTTAAATTTAATAAAGCCAAAAATTAGCTGTTGCAATAAAGGAGTAGAATATGTACTTG
1681 AAAGTAAAAGCTCAAAAGGTCAAAAAGATACGACCAACCGATGGATAAATTCCTGGCACCGGATGCATAT
1751 GCAGTTCATTCTCAAAAAACTTATTTGATATCATTTTGCCATTTTTAAAACATCTCTTGTTATATTGGTT
1821 CCAGAAGTTATACTCAGTTTAGCTAAGCATTGTATCTTCTTATAACGTAAGAATATTCAAGAAAATAGCTA
1891 CCCCATTAATAAAACTCTATCCGAACAATATGCGTTGTTGCCGACGATTCGTTTCTGTGATCATTTTGT
1961 CTAATTAAACCTAATGTAATTTTTTTAACTCCTGAAAATTATAATATTATTCCTATTTATATATATGTTC
2031 CCGGATTT
    
```

Fig. 3. Sequence of alkali myosin light chain gene of *S. digitata*. The nucleotide sequence of exons and the 5' and 3' flanking sequences are presented in capital letters while the intron sequences are in lower case. The predicted amino acid sequence, in single-letter terminology, is indicated below the nucleotide sequences. The potential CAAT box like sequence, CCAAT in the 5' flanking region and the polyadenylation signal AATAA in the 3' flanking region are boxed. Two EF hand domains are underlined with a single line.

The Southern blot analysis of the *S. digitata* genomic DNA revealed a single hybridization band in the lanes cleaved with *Bam*H1, *Hind*111 and *Sal* 1 while the lane cleaved with

*Eco*R1 resulted in two hybridization fragments as the alkali myosin light chain gene of *S. digitata* had one restriction site for *Eco*R1 and none for other enzymes used. The banding pattern of the Southern blot analysis remained same even

under low stringency conditions [Figure-4] suggesting that the alkali myosin light chain gene of *S. digitata* is likely to be a single copy gene. However, alternative splicing resulting in several isoforms cannot be excluded.

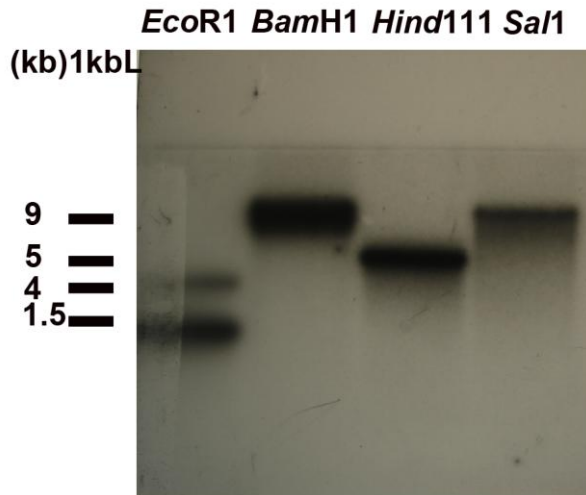


Fig. 4. Southern blot of *S. digitata* genomic DNA. *S. digitata* genomic DNA cleaved with *EcoR1*, *BamH1*, *Hind111* and *SalI* and probed with ^{32}P labeled *S. digitata* alkali myosin light chain cDNA sequences. 1 kb Ladder (1kb L) was used as the size marker

Analysis of the nucleic acid sequence of the entire coding region revealed a full open reading frame of 450 nucleotides. Translation of this full open reading frame encoded a putative 149 amino acid protein with the predicted molecular weight of 17 kD. Based on the results obtained from the PSORTII program, which predict the intracellular location of the proteins by known sequence fingerprints, the characterized alkali myosin light chain appears to be of cytoplasmic origin. The codon usage pattern of alkali myosin light chain gene of *S. digitata* revealed that only 50 codons were utilized out of the 61 codons. Certain amino acids showed a strong preference for a specific codon, GTT was used 60% in valine, TCA was used 43% in serine, GGA was used 61% in glycine.

In order to identify similar genes of other taxonomic groups a homology sequence search was done with NCBI database. A partial mRNA fragment of the human filarial parasite *B. malayi* [Acc No. XM_001894833] showed a high degree of homology of 90% at protein level. But this protein was denoted as one of the hypothetical protein of *B. malayi* because neither the complete mRNA nor the gene of the relevant protein was fully characterised. Next to that, a high degree homology of more than 80% was observed with free-living nematode *Caenorhabditis briggsae*.

The alignment of the homology sequences in order of decreasing homology is shown in [Figure-5]. The homology

was around 48-50% when compared with higher eukaryotes including the avian and mammalian species.

Thus, the alkali myosin light chain gene appears to be highly specific for nematodes and less conserved across the taxonomic groups unlike other genes like actin. Analysis of sequenced ESTs from 30 different nematode species across the phylum has shown that only about 15% of the genes common to all four clades of nematodes have sequence matches outside the phylum. In addition, they identified ~1300 genes that are nematode-specific found only in most of the nematodes [29]. Myosin light chain genes are reported to show a vast diversity not only between different genetic groups but also in different tissues within the same organism [30].

Many of these isoforms especially from the lower eukaryotes are not characterized yet. In some cases, the transcript of a single gene is alternatively spliced resulting in different isoforms [31]. The analysis of amino acid sequence with the NCBI conserved domain database [32] for interactive domain family revealed that the protein belongs to the calcium binding protein which contain one or several of EF hand domains.

Though the Ca^{2+} binding proteins such as calmodulin, troponin C, myosin light chains and parvalbumin have evolved from a common ancestor with four Ca^{2+} binding domains, the NCBI conserved domain database identified only two domains in *S. digitata* alkali myosin light chain gene [Figure-3]. Alkali myosin light chain genes from other eukaryotes also contain only two Ca^{2+} binding domains [33, 34]. The loss of other two domains is perhaps due to some evolutionary substitution of amino acids in the Ca^{2+} loop, which makes them functionally inactive. Detail analysis of this domain revealed that there were four acidic residues among its six ligating groups in the Ca^{2+} loop to make it functionally active. Ca^{2+} binding EF hand conserved domain region of *S. digitata* alkali myosin light chain extending from amino acids 80 to 112 is highly conserved with the ancestral Ca^{2+} binding domain of higher eukaryotes although only around 48-50% amino acid homology was seen when the whole protein was compared [Figure-6].

[IV] CONCLUSION

In the present study, we have characterised the alkali myosin light chain gene of the cattle filarial parasite *S. digitata*. Since this is the first alkali myosin light chain gene characterised from filarial parasites, this will probably be helpful in the study of the same gene in related human filarial parasite *W. bancrofti* specially in designing PCR primers and DNA probes targeting this gene. Moreover, being one of the structural components of the cuticle, this myosin and myosin related proteins could be specifically focused as targets for novel vaccines and therapeutic agents. Further studies to express the protein for investigating the immunogenic potential would be desirable.

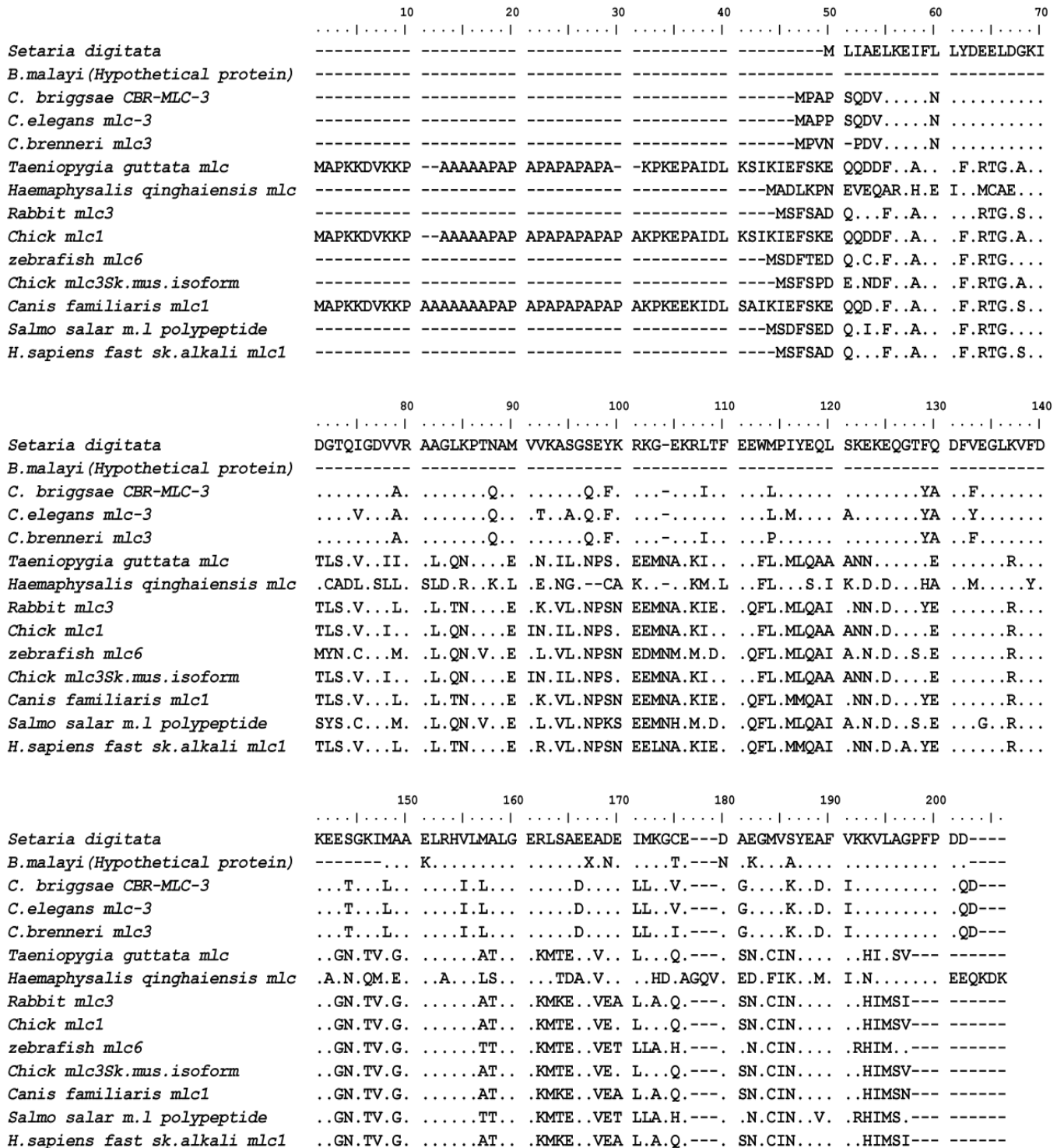


Fig: 5. Alignment of the highly similar deduced amino acid sequences of nematode alkali myosin light chain mlc-3 proteins with *S. digitata* in order of decreasing homology. The sequences were obtained from the protein database at NCBI. Residues identical to the consensus are indicated by dots. Gaps are indicated by hyphen.

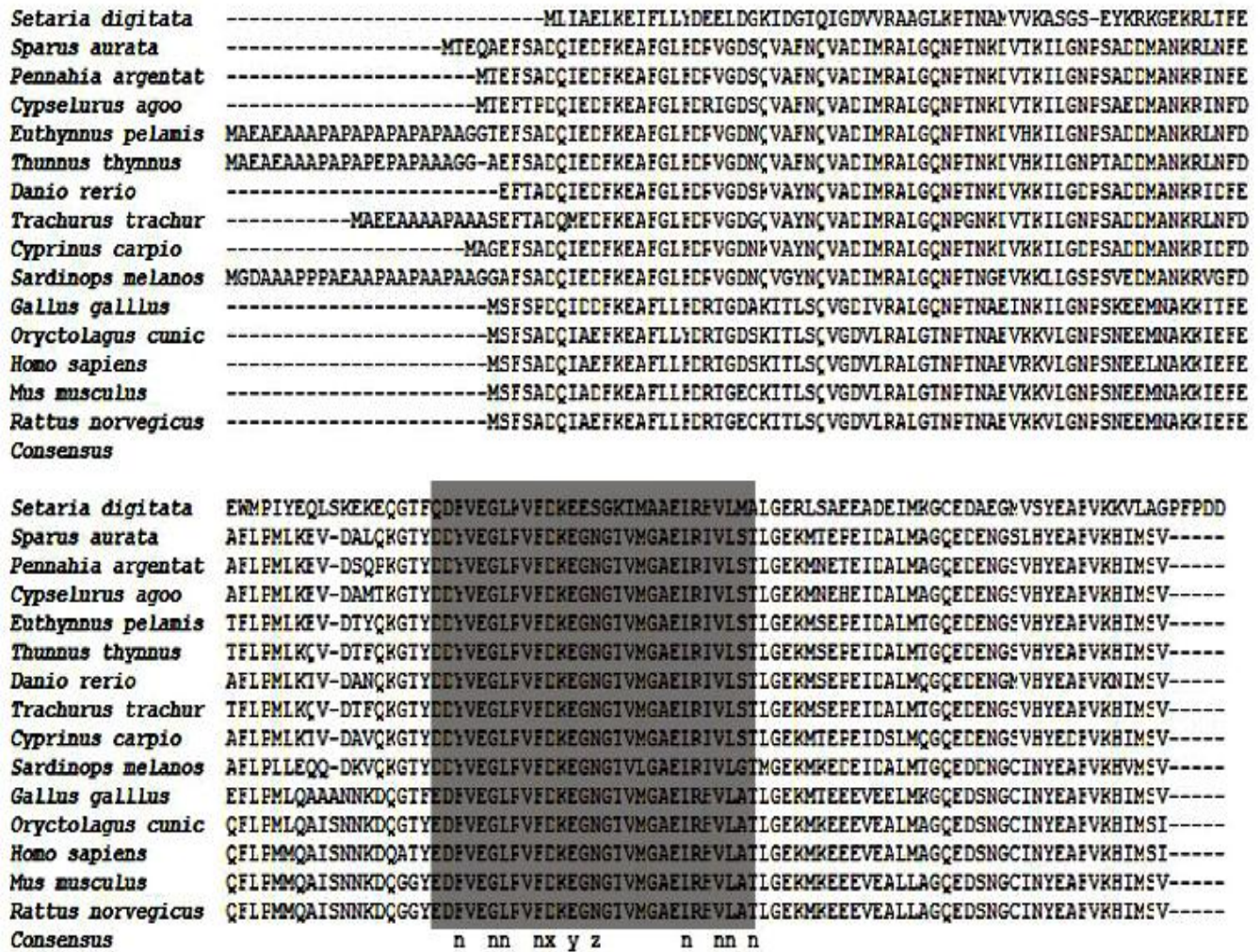


Fig: 6. Alignment of avian and mammalian myosin light chain (MLC3) amino acid sequences with *S. digitata*. The MLC3 specific domain of avian and mammalian sequences and the ancestral Ca²⁺ binding domain are indicated in shaded box. n indicates those residues which form the core of the E and F α helices. X, Y, Z, -X,-Y and -Z are residues which might be involved in the binding of divalent metal ions in EF hand domain.

FINANCIAL DISCLOSURE

This project was supported by the Swedish Agency for Research Cooperation with Developing Countries Grant for Molecular Biology and Biotechnology awarded to EHK and KHT and constituted part of the MPhil programme of MA.

CONFLICT OF INTERESTS

There is no financial or personal interest that might pose a conflict.

ACKNOWLEDGEMENT

We thank Mr. M Wickramanayeke for establishing the cDNA library and Prof. R. P. V. J. Rajapakse, Faculty of Veterinary Medicine and Animal Science for assistance in collecting *S. digitata* worms.

REFERENCES

- [1] Innes JRM, Shoho C, Pillai CP. [1952] Epizootic cerebrospinal nematodiasis of Setariasi. *Brit Vet J* 108:71–88.
- [2] Gunawardena GSP de S. [1991] Studies on cerebrospinal nematodiasis in sheep and goats in Sri Lanka. Ph.D Thesis, University of Peradeniya, Sri Lanka.
- [3] Jayasena SMT, Chandrasekaran NV, Karunanayake EH. [1999] Molecular characterisation of a hsp70 gene from the filarial parasite *Setaria digitata*. *Int. J Parasitolol* 29:581–591.
- [4] Molyneux DH, Bradley M, Hoerauf A, Kyelem D, Taylor MJ. [2003] Mass drug treatment for lymphatic filariasis and onchocerciasis. *Trends Parasitol* 19: 516 – 522.
- [5] Goldman AS, Guisinger VH, Aikins M, Amarillo MLE, Belizario VY, Garshong B, Gyapong J, Kabali C, Kamal HA, Kanjilal S, Kyelem D, Lizardo J, Malecela M, Mubyazi G,

- Nitie'ma PA Ramzy RMR, Streit TG, Wallace A, Brady MA, Rheingans R, Ottesen EA, Haddix AC. [2007] National Mass Drug Administration Costs for Lymphatic Filariasis Elimination. *PLoS Negl Trop Dis* 1(1): e67.
- [6] World Health Organisation [1992] Lymphatic Filariasis: the disease and its control. *Fifth report of the WHO expert committee on filariasis. WHO, Geneva.*
- [7] Decruse W, Raj KR. [1990] Histological studies of female *Setaria digitata* (Von Linstove 1906) a filarial of Bovine, *Bos indicus*. *P Indian As-Anim Sci* 99: 103–112.
- [8] Dissanayeke S, Ismail MN. [1980] Antigens of *Setaria digitata* cross reaction with surface antigens of *Wuchereria bancrofti* microfilaria and serum antibodies in *W.bancrofti* infected subjects. *Bull WHO* 58: 649–654.
- [9] Falkenthal S, Parker VP, Davidson N. [1985] Developmental variations in the splicing pattern of transcripts from the *Drosophila* gene encoding myosin alkali light chain result in different carboxyl-terminal amino acid sequences. *P Natl Acad Sci U S A* 82: 449–453.
- [10] Sasisekhar B, Suba N, Sindhuja S, Sofi GMA, Narayanan RB. [2005] *Setaria digitata*: Identification and characterisation of hypodermally expressed SXP/RAL2 protein. *Exp Parasitol* 111: 121–125.
- [11] Raghavan N, McReynolds LA, Maina CV, Feinstein SM, Jayaratnam K, Ottesen EA, Nutman TB. [1991] A recombinant clone of *Wuchereria bancrofti* with DNA specificity for human lymphatic filarial parasites. *Mol Biochem Parasitol* 47: 63–71.
- [12] Langy S, Plichart C, Luquiaud P, Williams SA, Nicolas L. [1998] The immunodominant *Brugia malayi* paramyosin as a marker of current infection with *Wuchereria bancrofti* adult worms. *Infect Immun* 66: 2854–2858.
- [13] Verma SK, Bansal I, VEDI S, Saxena JK, Katoch VM, Bhattacharya SM. [2008] Molecular cloning, purification and characterisation of myosin of human lymphatic filarial parasite *Brugia malayi*. *Parasitol Res* 102: 481–489.
- [14] Wickramanayake MN, Ekanayake S, Karunayake EH. [2001] *Wuchereria bancrofti*: detection of microfilaria in asymptomatic microfilaraemic individuals with *Setaria digitata* antigens. *Southeast Asian J Trop Med Public Health* 32: 230 – 234.
- [15] Wickramanayake MN, Chandrasekaran NV, Ekanayake S, Karunayake EH. [1998] A *Setaria digitata* cDNA clone encoding the gene for myosin light chain recognised by sera from patients with Bancroftian filariasis. *Proceedings of the fifty fourth annual Session for the Sri Lanka Association for the Advancement of Science*, 36: 28
- [16] Wijesundera, WSS, Chandrasekaran NV, Karunanayake EH, Rajapakse RPVJ. [1997] Development of a rapid, nonradioactive, oligonucleotide-based assay for the detection of *Setaria digitata*. *Exp Parasitol*. 86:161–162.
- [17] Sambrook J, Fitch EF, Maniatis T. [1989] Molecular Cloning: A Laboratory Manual. Cold Spring Harbor, Cold Spring Harbor Press, 13: E3–E4.
- [18] Saverimuttu JKS, Karunanayake EH, Chandrasekaran NV, Jayasena SMT. [2000] Molecular characterisation of the actin gene of the filarial parasite *Wuchereria bancrofti*. *Int J Parasitol* 30: 119–124
- [19] <http://www.ncbi.nlm.nih.gov/gorf/gorf.html>
- [20] <http://blast.ncbi.nlm.nih.gov/Blast.cgi>
- [21] <http://www.ncbi.nlm.nih.gov/Structure/cdd/wrpsb.cgi>
- [22] <http://psort.hgc.jp/form2.html>
- [23] Prestridge DS. [1991] SIGNAL SCAN: A computer program that scans DNA sequences for eukaryotic transcriptional elements. *CABIOS* 7, 203–206. <http://www.bimas.cit.nih.gov/molbio/signal/>
- [24] Hammond MP, Bianco AE. [1992] Genes and genomes of parasitic nematodes. *Parasitol Today* 8:299–30
- [25] Kovaleva ES, Subbotin SA, Masler EP, Chitwood DJ. [2005] Molecular characterisation of the actin gene from cyst nematodes in comparison with those from other nematodes. *Comp Parasitol* 72: 39–49
- [26] Breathnach R, Chambon P. [1981] Organisation and expression of eukaryotic split genes coding for proteins. *Ann Rev Biochem* 50: 349–383
- [27] Cohen A, Barton PJR, Robert B, Garner I, Alonso S, Buckingham ME. [1998] Promoter analysis of myosin alkali light chain genes expressed in mouse striated muscle. *Nucleic Acids Res* 16: 10037–10052.
- [28] Glockner G. [2000] Large scale sequencing and analysis of AT rich eukaryotic genomes. *Genomics* 1: 289–299
- [29] Parkinson J, Mitreva M, Hall N, Blaxter M, McCarter JP. [2003] 400 000 nematode ESTs on the Net. *Trends Parasitol* 19: 283–286
- [30] Scott L, Hooper, Thuma JB. [2005] Invertebrate Muscle: Muscle specific genes and proteins. *Physiol Rev* 85: 1001–1060
- [31] Goodwin EB, Szent-Gyorgyi AG, Leinwan LA. [1987] Cloning and characterisation of the scallop essential and regulatory myosin light chain cDNA. *J Biol Chem*, 262: 11052–11056.
- [32] Marchler-Bauer A, Anderson JB, Derbyshire MK, DeWeese-Scott C, Gonzales NR, Gwadz M, Hao L, He S, Hurwitz DI, Jackson JD, Ke Z, Krylov D, Lanczycki CJ, Liebert CA, Liu C, Lu F, Lu S, Marchler GH, Mullokanov M, Song JS, Thanki N, Yamashita RA, Yin JJ, Zhang D, Bryant SH. [2006] CDD: A conserved domain database for interactive domain family analysis. *Nucleic Acids Res* 35: D237–D240
- [33] Moutou KA, Canario ANM, Mamuris Z, Power DM. [2001] Molecular cloning and sequencing of *Sparus aurata* skeletal myosin light chains expressed in white muscle: developmental expression and thyroid regulation. *J Exp Biol* 204: 3009–30018
- [34] Gao J, Luo J, Luo, Fan R, Guan G, Ren Q, Ma M, Sugimoto C, Bai Q, Yin H. [2007] Molecular characterisation of a myosin alkali light chain –like protein, a “concealed” antigen from the hard tick *Haemaphysalis qinghaiensis*. *Vet Parasitol* 147: 140–149.

ABOUT AUTHORS



Prof. Eric H Karunayake is Emeritus Professor of Biochemistry and Founder Director of the Institute of Biochemistry, Molecular Biology and Biotechnology (IBMBB), University of Colombo. He has been involved in the study of molecular biology of Filarial parasites for more than two decades.



Prof. Kamani H Tennekoon is the Professor of molecular Life sciences and Director of the IBMBB, University of Colombo. She formerly held the chair of physiology at the Faculty of Medicine, University of Colombo. Her main research is in Reproductive and Developmental molecular Biology.



Dr. A. Muruganathan is a Lecturer attached to Faculty of Medicine, University of Jaffna, Sri Lanka, presently reading for his postgraduate studies at the IBMBB, University of Colombo, in the field of Molecular Parasitology specifically on the characterisation of filarial parasite specific genes.

UNFOLDING SIMULATIONS OF COLD- AND WARM-ADAPTED ELASTASES

Laura Riccardi¹, Papaleo Elena²*¹Biomolecular Dynamics Laboratory, Institute of Physics, Albert Ludwigs University, Freiburg, GERMANY²Department of Biotechnology and Biosciences, University of Milano-Bicocca, Milan, ITALYReceived on: 9th-July-2010; Revised on: 8th-Sept-2010; Accepted on: 14th-Oct-2010; Published on: 8th-Nov-2010.*Corresponding author: Email: elena.papaleo@unimib.it Tel: +39-0264483475; Fax: +39-0264483478

ABSTRACT

The earth surface is dominated by low temperature environments, which have been successfully colonized by several extremophilic organisms. Enzymes isolated from psychrophilic organisms are able to catalyze reactions at low temperatures at which enzymes from mesophiles or thermophiles are fully compromised. The current scenario on enzyme cold-adaptation suggest that these enzymes are characterized by higher catalytic efficiency at low temperatures, enhanced structural flexibility and lower thermostability. In the present contribution, molecular dynamics simulations in explicit solvent have been carried out at different high temperatures in order to investigate the unfolding process of cold- and warm-adapted homologous enzymes. In particular, we focused our attention on cold-adapted elastases for which it was previously demonstrated that the psychrophilic enzyme presents higher localized flexibility in loops surrounding the catalytic site and the specificity pocket. The unfolding simulations show a slower unfolding process for the cold-adapted enzyme, but characterized by a greater loss of intramolecular interactions and α -helices than the mesophilic counterparts.

Keywords: cold-adapted enzymes; unfolding; molecular dynamics simulations; psychrophilic enzymes; elastase; serine-protease

[1] INTRODUCTION

In recent years, increasing interest has been devoted to the investigation of determinants of adaptation to low temperatures of the enzymatic repertory of cold-adapted organisms [1, 2]. The study of cold-adapted enzymes attracts both fundamental researches than industrial application for the design of new biocatalysts [3, 4]. The number of reports on enzymes from psychrophilic organisms has increased over the past years, and reveals that adaptative strategies vary among different enzymes, which use different structural features for gaining increased catalytic efficiency at low temperatures, reduced thermal stability and increased molecular flexibility.

In fact, enzyme catalysis generally involves the “breathing” of particular protein regions, enabling the accommodation of the substrate [1]. The optimization of enzyme function at a given temperature requires a proper balance between two opposing factors: structural rigidity, allowing the retention of a specific conformation at the physiological temperature, and flexibility, allowing the protein to perform its catalytic function [5].

Whereas heat-adaptation seems to be generally related to protein rigidity, cold-adaptation, at the opposite side of the

temperature scale, should be characterized by enhanced flexibility of crucial protein regions in order to compensate for the lower thermal energy in low temperature habitats [6, 7]. This plasticity has been suggested to enable a good complementarity with the substrate at a low energy cost. In return, this flexibility would be responsible for the high thermostability of the psychrophilic enzymes. The low stability of psychrophilic enzymes has been demonstrated by the drastic shift of their apparent optimal temperature of activity, the low resistance of the protein to denaturing agents and the high propensity of the structure to unfold at moderate temperatures [1].

High temperature MD simulations turned out a valuable tool to study unfolding process of several protein systems [8-12]. In particular, all-atom explicit solvent MD simulations provide insights into biomolecules dynamics thanks to the continuity of the trajectory in the phase space and are a useful tool to complement experimental investigations. MD can provide further information on the protein folding and unfolding processes along with elucidation of intermediates and factors affecting stability of folded and unfolded forms [8, 13-14].

Protein unfolding studies by atomistic simulations are carried out generally increasing the temperature necessary to overcome the enthalpic forces stabilizing the three-dimensional structure. It has been demonstrated that high temperature simulations accelerate the unfolding pathway without affecting the pathway itself [15]. The use of higher temperatures over the unfolding experimental temperatures is necessary considering the differences in the time scales accessible by experiments and calculations. In MD simulations at high temperatures, protein unfolding can occur within a few nanoseconds [15-16].

In light of the above observations, we decided to investigate the thermal unfolding process of a mesophilic and cold-adapted elastases by multiple-*replica* MD simulations. The aim of this study is not only to analyze specific features of the unfolding mechanisms of the two homologous elastases, but also to gain a deeper understanding of molecular basis of cold-adaptation of psychrophilic serine proteases, which at low temperatures are known to be characterized by higher catalytic activity [17] and higher local structural flexibility in the proximity of the functional sites [6], with respect to the mesophilic counterpart.

[II] MATERIALS AND METHODS

MD simulations were performed using the GROMACS software and GROMOS96 force field (www.gromacs.org) implemented on a parallel architecture. The enzymes selected for this study have been the mesophilic pancreatic porcine (PE) and psychrophilic Atlantic salmon (SE) elastases (PDB entries 1LVY and 1ELT, respectively). For these enzymes various MD simulations were previously carried out at 283 and 310K [6]. In particular, for both the warm and cold-adapted elastase, we selected two structures from two different independent simulations at 310 K. These structures are representative of the conformational space explored at this reference temperature. To reach the desired unfolding temperatures, solvent have been equilibrated in 4 steps increasing the temperature at each step (310→350, 350→400, 400→450, 450→500 K), during which the protein atomic positions were restrained using a harmonic potential. In the simulations, the structures were soaked in a dodecahedral box of SPC (Simple Point Charged) water molecules and simulations were carried out using periodic boundary conditions. The ionization state of the residues was set to be consistent with neutral pH and tautomeric form of histidine residues was derived using GROMACS tools and confirmed by visual inspection. Cl⁻ counterions were added to neutralize the system.

Productive MD simulations were performed in the isothermic-isobaric ensemble (NPT ensemble) at 400, 450 and 500K, applying periodic boundary conditions and using an external bath with a coupling constant of 0.1 ps. Pressure was kept constant at 1 atm and the time-constant for the pressure coupling was set to 1 ps. The LINCS algorithm was used to constraint bond lengths, allowing to use a 2 fs time step. Electrostatic interactions were calculated using the Particle-mesh Ewald (PME) summation scheme. Van der Waals and Coulomb interactions were truncated at 1.0 nm. The nonbonded pair list was updated every 10 steps and conformation stored every 2ps.

To improve the conformational sampling, independent simulations (*replicas*) obtained initializing the MD runs with different Maxwellian distributions of initial velocities, were carried out for each protein system at each temperature. In particular, two and four 3 ns simulations have been carried out at 400K and 450-500K, respectively. The different simulations have been identified according to different codes.

The two letters (PE-SE) identify the enzyme, the number (400-450-500) is referred to the simulation temperature, the roman number (III-IV) defines the two different initial structures whereas the last letter (a-b) discriminates between the different initial velocities.

For example, PE450IIIa and PE450IIIb refer to simulations of the porcine elastase at 450K performed starting from the same initial structure but with a different initial random seed (a and b), whereas PE450IIIa and PE450IVa refer to simulations of the porcine elastase at 450K performed starting from two different initial structures (III and IV).

[III] RESULTS

Unfolding simulations of a cold-adapted elastase (SE) and its mesophilic counterpart (PE) have been carried out in order to shed light on molecular characteristics of cold-adaptation.

Generally, each protein molecule may unfold via its own pathway and, though the majority of the pathways are probably similar, some of them may differ from other considerably. Therefore, to ensure the validity of unfolding simulations and that the main traits of the trajectories are reproducible and representative, it is necessary to analyse multiple trajectories related to the same system.

3.1. Unfolding profiles

A measure to identify the unfolded state is the RMSD (root mean square deviation) with respect to a reference structure. It is generally accepted that mainchain RMSD > 5 Å, calculated using as reference structure the native structure, defines that the protein is in an unfolded state [18]. RMSD values were calculated on mainchain atoms using as a reference the starting structure of the simulations [Figure-1].

The most evident changes in the elastase native structure are detected at 500K, even if structural changes can be already identified at 400K simulations. At 500K, the mesophilic enzyme undergoes a greater structural rearrangement, presenting a fast unfolding of the structure, after which seems to reach an equilibrium state. In SE the trend is more linear: the increase in RMSD is slower and on-going.

Another parameter reflecting structural changes is the protein radius of gyration (R_g), which is a measure of compactness of the protein structure. However, it is not sufficiently informative if considered alone, since in the unfolded state a protein could still retain some degree of compactness. Therefore, two-dimensional plot of mainchain RMSD versus protein radius of gyration have been carried out, also in order to remove the differences due to the fact that corresponding events could occur at different times in different trajectories [Figure-2, 3]. Different colors indicate three different parts of the simulations: black, red and green correspond to the first 1ns, from 1 to 2 ns, and from 2 to 3 ns, respectively. Some trajectories show an approximately simultaneous increase in R_g and RMSD in the first part of the unfolding process and much more complexity after partial denaturation, whereas others have a complex behavior starting from the initial stages of the unfolding process.

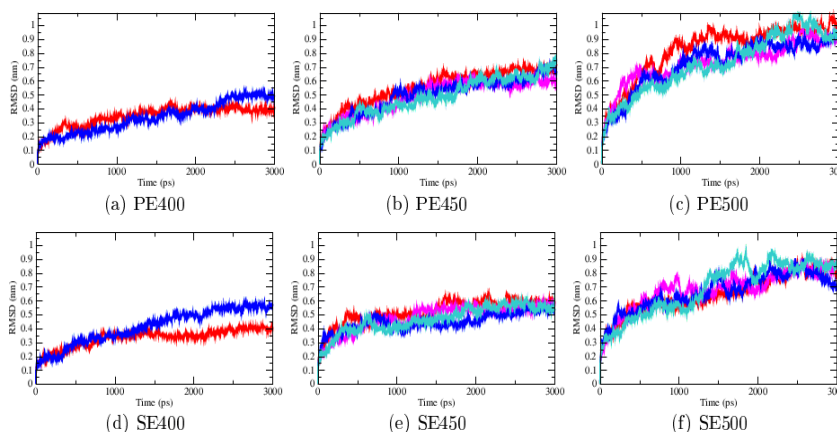


Fig 1. RMSD as a function of simulation time. The different colors indicate the different independent simulations for each system.

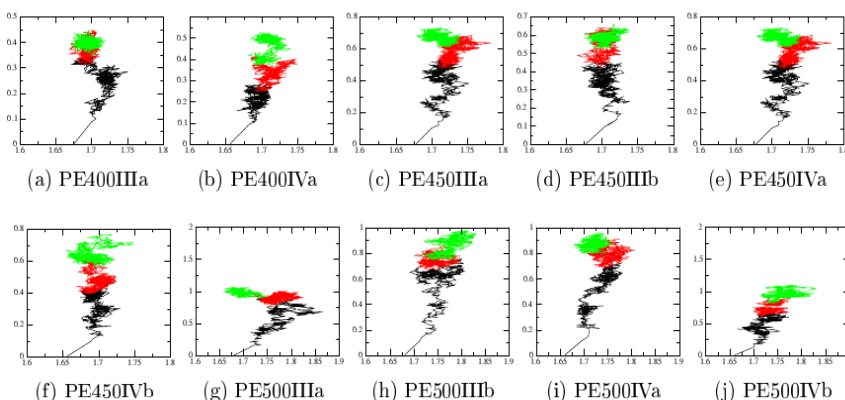


Fig 2. Rg (x-axis) versus Rmids (y-axis) in PE simulations. The different colors indicate different simulation time windows (black 0-1ns, red 1-2 ns and green 2-3 ns).

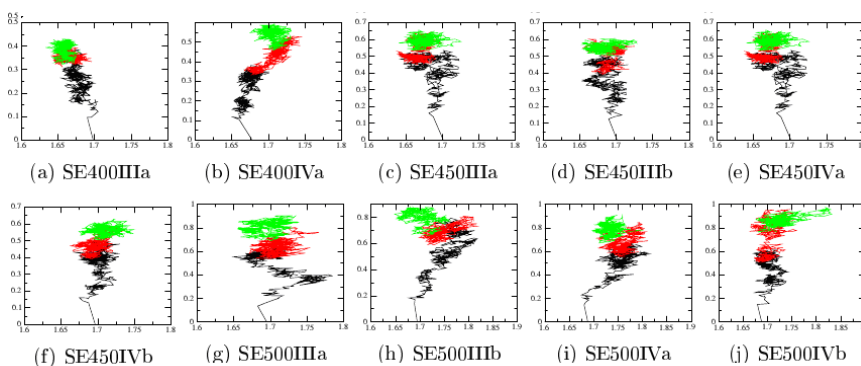


Fig 3. Rg (x-axis) versus Rmids (y-axis) in SE simulations. The different colors indicate different simulation time windows (black 0-1ns, red 1-2 ns and green 2-3 ns).

3.2. RMSD matrices

In order to understand if there are common features in the unfolding pathway, all the structures of each simulations at a given temperature have been compared, measuring mainchain

RMSD, with the structures of other simulations at the same temperature (for example, simulations a versus b) [Figure-4] and with the simulations at the other temperatures but performed from the same starting structures (for example simulation at 400K versus 500K) [Figure-4].

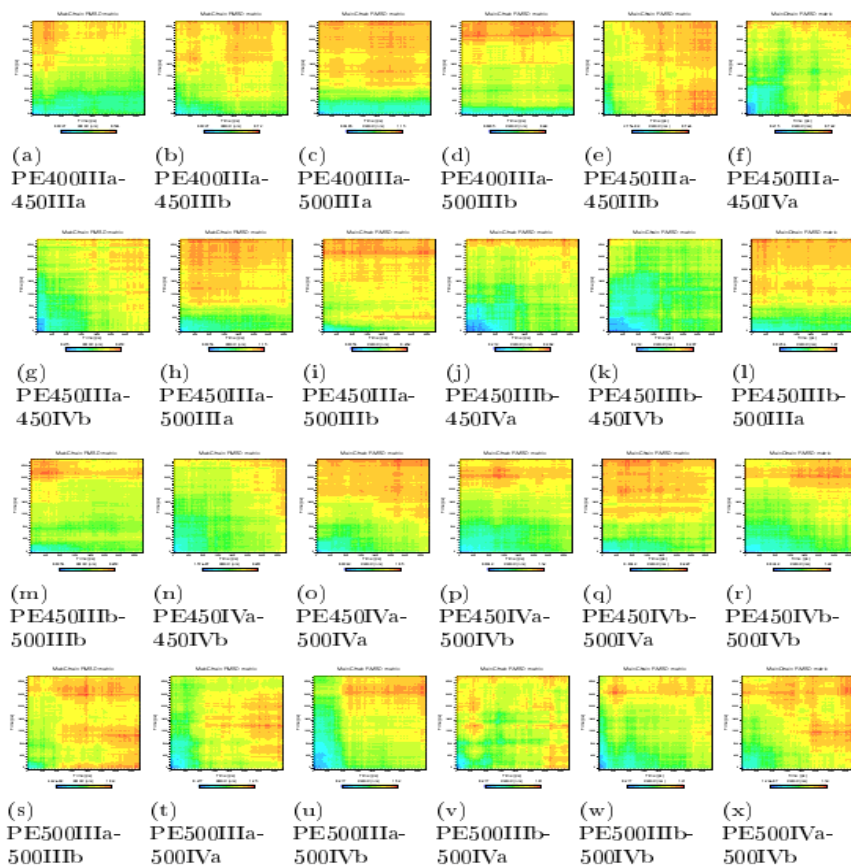


Fig 4. RMSD matrices of PE. The matrices present the RMSD obtained from the comparison of each structure of a simulations with the structures collected from another simulation. Both comparisons of independent replicas of the same system at the same temperature and of replicas of the same system at different temperatures are shown. The RMSD matrices of SE simulations present a comparable trend (*data not shown*). The color bar indicate increasing RMSD values from blue to red.

In particular, the RMSD matrices are computed calculating the mainchain RMSD between all the structures of one simulation (x-axis) against all the structures of another simulation (y-axis). A color scale from blue to red indicates increasing values of RMSD. A blue area means that corresponding structures in the two simulations have an high degree of similarity.

Comparing simulations at the same temperature, the highest similarity is gathered in the left-low corner. Following the simulation course, simulations performed using different starting structures and different initial atomic velocities, drift away from each other.

In **Figure-4**, cyan indicates low RMSD values and structural similarity is concentrate in the lower rows of the matrices. The x-axis corresponds to the simulation at the lower temperature, indicating that at 500K the protein follows the same pathway explored at 400K, but employing less computational time. The high temperature seems not affect the unfolding pathway itself since the structures collected in the initial steps of 500K simulations resemble structures from 400K simulations, but only speed up the process.

3.3. Intramolecular interactions and secondary and tertiary structure content.

The numbers of intramolecular hydrogen bonds (H-bonds) have been monitored along the simulation time. Even if the total number is not informative in terms of individual residues involved in the interactions, it can give an estimation of the compactness of the structures and the lack of native structures. It turns out that at 500K the number of H-bonds is clearly reduced. In fact, at 500K PE and SE has an average value of H-bonds of 110 and 100, respectively, whereas the native structure is characterized by 185 and 182 H-bonds, respectively [6]. In particular, in PE the H-bonds decrease till 2 ns and then increase again at the end of the simulations, suggesting the breaking of native intramolecular interactions and formation of non-native intramolecular interactions in the unfolded state. Whereas in the native structure SE and PE present a almost comparable number of total intramolecular H-bonds, SE tends to lose a higher number of H-bonds that PE in the early step of the unfolding process. In fact, average H-bonds in the first 500 ps of simulation at 500K are reduced to 104 in SE and 120 in PE.

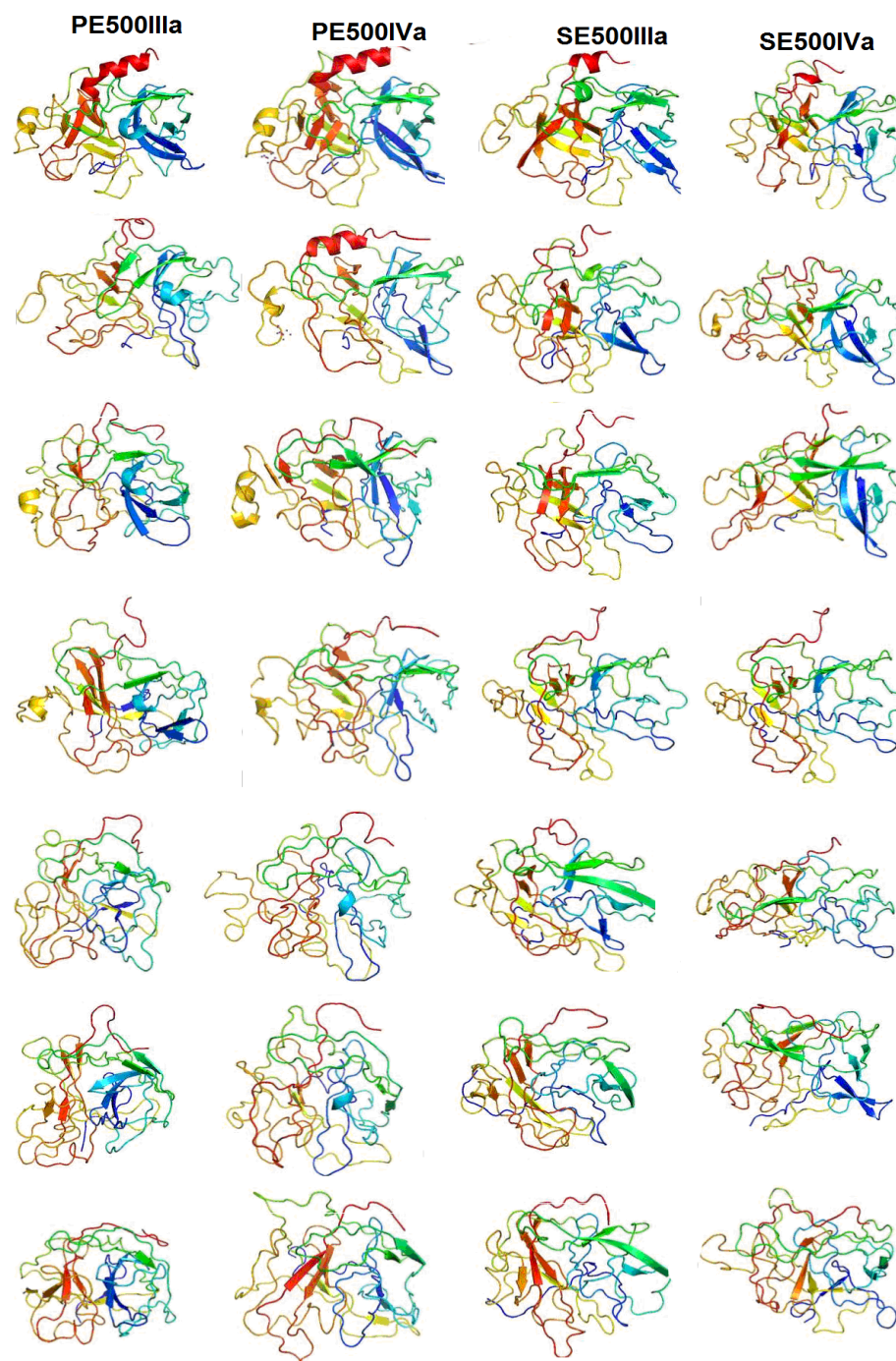


Fig 5. Snapshots taken from simulations at 500K every 0.5 ns. Data relative to simulations at 500 K are indicated. The different columns correspond to PEIIIa, PEIVa, SEIIIa and SEIVa, respectively.

3D structure of elastases folds into two juxtaposed domains characterized by an antiparallel β -type fold, including some α -helices. Secondary structure content over the simulation time have been also monitored, according to the DSSP program definition [19] as well as snapshots from the simulations

[Figure-5]. The starting conformations of the mesophilic enzyme are always more structured in β -sheet, for at least 20 residues more, than the psychrophilic counterpart.

At 400K, both in PE and SE the changes in the structures are quite slow, in agreement with the RMSD analysis. Interestingly, the reduction in residues involved in α -helices is a common feature of the two enzymes at both temperatures. However, SE tends to lose α -helices in the earlier steps than PE. In fact, in SE α -helix content is reduced of more of more that 75% just after 0.1 ns, whereas PE retains native α -helices up to 0.5 ns. At this temperature systems are not completely unfolded. More interestingly, at 500K PE unfolds rapidly, in less than 0.4 ps the decrease of all structured residues is about 30% with respect to the native structure. After this early event, the secondary structure composition remains quite stable, in agreement with the previous indications by RMSD analysis. The psychrophilic enzyme presents a slower unfolding process with the main transition appearing in the range between 0.4 and 1 ns. In both systems, β -sheet conformations, which are the main component of the native elastase 3D fold, seem to be fairly stable in the first step of the unfolding process and decrease in the last ns.

[IV] CONCLUSION

In the present contribution, we present an investigation at the molecular level of the unfolding process of two homologous enzymes sharing a common fold and a high sequence similarity (more than 68% of sequence identity) but adapted to different temperature conditions. Both enzymes present in the first steps of the unfolding process a loss of native α -helices. At 500K the unfolding process is clearly visible: after only 0.4 ns the mesophilic enzyme has lost 30% of the native structures. The unfolding process in the psychrophilic enzyme occurs later, in agreement with a higher flexibility and lower number of intramolecular interactions localized in the proximity of the functional site but a higher rigidity of the rest of the protein structure with respect to the mesophilic counterpart [6]. Interestingly, even if SE seems from our simulations to undergo toward a slower unfolding process, the regions in the proximity of the catalytic triads are the first to be affected by increased temperatures and promote the local unfolding in the first step of the process.

FINANCIAL DISCLOSURE

The work has been supported by computational facilities at Cineca (Project-562 and Project-609) and CASPUR Standard HPC-Grant 2010.

ACKNOWLEDGEMENT

The authors thank Prof. Luca De Gioia for fruitful discussion and comments.

REFERENCES

- [1] Siddiqui KS, Cavicchioli R. [2006] Cold-adapted enzymes. *Annu Rev Biochem* 75: 403–433.
- [2] D'Amico S, Collins T, Marx JC et al. [2006] Psychrophilic microorganisms: challenges for life. *EMBO Rep* 7: 385–389.

- [3] Gerday C, Aittaleb M, Bentahir M et al. [2000] Cold-adapted enzymes: from fundamentals to biotechnology. *Trends Biotechnol* 18: 103–107.
- [4] Tutino ML, di Prisco G, Marino G et al. [2009] Cold-adapted esterases and lipases: from fundamentals to application. *Protein Pept Lett* 16: 1172–1180.
- [5] Fields PA. [2001] Review: Protein function at thermal extremes: balancing stability and flexibility. *Comp Biochem Physiol A Mol Integr Physiol* 129: 417–431.
- [6] Papaleo E, Riccardi L, Villa C et al. [2006] Flexibility and enzymatic cold-adaptation: a comparative molecular dynamics investigation of the elastase family. *Biochim Biophys Acta* 1764: 139–1406
- [7] Chiuri R, Maiorano G, Rizzello A et al. [2009] Exploring local flexibility/rigidity in psychrophilic and mesophilic carbonic anhydrases. *Biophys J* 96: 1586–1596.
- [8] Day R, Daggett V. [2003] All-atom simulations of protein folding and unfolding. *Adv Protein Chem* 66: 373–403.
- [9] Olufsen M, Brandsdal BO, Smalås AO. [2007] Comparative unfolding studies of psychrophilic and mesophilic uracil DNA glycosylase: MD simulations show reduced thermal stability of the cold-adapted enzyme. *J Mol Graph Model* 26: 124–134.
- [10] Kundu S, Roy D. [2008] Temperature-induced unfolding pathway of a type III antifreeze protein: insight from molecular dynamics simulation. *J Mol Graph Model* 27: 88–94.
- [11] Jonsson AL, Scott KA, Daggett V. [2009] Dymeomics: a consensus view of the protein unfolding/folding transition state ensemble across a diverse set of protein folds. *Biophys J* 97: 2958–2966.
- [12] Priyakumar UD, Ramakrishna S, Nagarjuna KR et al. [2010] Structural and energetic determinants of thermal stability and hierarchical unfolding pathways of hyperthermophilic proteins, Sac7d and Sso7d. *J Phys Chem B* 114: 1707–1718.
- [13] Fersht AR, Daggett V. [2002] Protein folding and unfolding at atomic resolution. *Cell* 108: 573–582.
- [14] Hansia P, Dev S, Suroliya A et al. [2007] Insight into the early stages of thermal unfolding of peanut agglutinin by molecular dynamics simulations. *Proteins* 69: 32–42.
- [15] Day R, Bennion BJ, Ham S et al. [2002] Increasing temperature accelerates protein unfolding without changing the pathway of unfolding. *J Mol Biol* 322: 189–203.
- [16] Daggett V. [2002] Molecular dynamics simulations of the protein unfolding/folding reaction. *Acc Chem Res* 35: 422–429.
- [17] Berglund GI, Smalås AO, Outzen H et al. [1998] Purification and characterization of pancreatic elastase from North Atlantic salmon (*Salmo salar*). *Mol Mar Biol Biotechnol* 7: 105–114.
- [18] Sham YY, Ma B, Tsai CJ et al. [2001] Molecular dynamics simulation of Escherichia coli dihydrofolate reductase and its protein fragments: relative stabilities in experiment and simulations. *Protein Sci* 10: 135–148.
- [19] Kabsch W, Sander C. [1983] Dictionary of protein secondary structure: pattern recognition of hydrogen-bonded and geometrical features. *Biopolymers* 22: 2577–2637.

ABOUT AUTHORS



Laura Riccardi has been a Master Student in Bioinformatics at the Molecular Modelling Laboratory of the Department of Biotechnology and Biosciences (University of Milano-Bicocca), studying determinants of cold-adaptation in psychrophilic elastases. She is presently a PhD student at the Biomolecular Dynamics Laboratory (University of Freiburg) under the supervision of Prof. G. Stock. Her project focuses on simulations of RNA systems, with particular attention to the characterization of the free-energy landscape and the study of the effects of small ligands on functional RNAs.



Dr. Elena Papaleo, PhD, is presently Young Researcher at the Molecular Modelling Laboratory of the Department of Biotechnology and Biosciences (University of Milano-Bicocca). Her research focuses on structure-function relationship in several protein systems by computational simulations. In particular, she has consolidated experience in the structural investigation of enzymes isolated from cold-adapted organisms. In her career, she has been main author or co-author of 18 scientific articles and 2 reviews.

SHORT COMMUNICATION: BIOTECHNOLOGY

APPLICATION OF PROTEASE FROM BACILLUS CEREUS MCM B-326 AS A BATING AGENT IN LEATHER PROCESSING

Vasudeo Zambare, Smita Nilegaonkar* and Pradnya Kanekar

Microbial Sciences Division, Agharkar Research Institute, G. G. Agarkar Road, Pune, Maharashtra 422403, INDIA

Received on: 11th -Sept-2010; Revised on: 28th -Oct-2010; Accepted on: 30th -Oct-2010; Published on: 12th -Nov-2010.

*Corresponding author: Email: ssnilegaonkar@gmail.com, Tel: 91-020-25654357

ABSTRACT

Laboratory scale experiments were carried out to test the efficiency of the extracellular protease from *Bacillus cereus* MCM B-326; cattle dung and commercial bate powder (ComBate) as bating agents on delimed buffalo hide. Protease treated pelt was free from scud and pigments, clean and fine grain, white, smooth and silkier with loosen fat. Histological sections of bated pelts showed greater opening up of collagen fibers with *Bacillus protease*. The studies indicated potential importance of *Bacillus protease* as effective bating agent in leather processing.

Keywords: *Bacillus cereus*; protease; bating agent; buffalo hide; leather processing

[I] INTRODUCTION

Enzymes have considerable potential in the bioprocessing of skins and hides for leather production, offering effective biotreatments particularly for the dehairing and bating processes [1]. The six processing steps viz. curing, soaking, dehairing, bating, degreasing and tanning are clearly identified steps in the preparation of leather [2]. In soaking, dehairing, bating and degreasing steps enzymes play an important role. It is common knowledge that, of the various unit operations involved in making leather, it is only with bating that the enzymatic process can't be substituted by chemical method. Bating is the treatment of dehaired hides or skins with an aqueous solution of an enzyme to remove certain undesirable proteinaceous constituents [3]. The main function of bating was the removal of and hydrolysis of the keratose substance remaining on the surface of the delimed pelt, i.e. removal of scud. The scud consists of epidermis, hair roots, pigments, fats, sebaceous glands and sweat gland debris [4]. Bating following the dehairing process produces softer, stretchier, silkier leather. Bating process acts on elastin and increase suppleness, pliability, elasticity and feel of the leather [5]. Depending on its proposed use like cloths, car seats etc. different enzyme treatments may be necessary. Puvankrishnan & Dhar reported several *Bacillus* sp. as a source of bating enzyme [6]. Three types of enzymes used as bating agents are (i) pancreatic protease i.e. trypsin from bovine and swine pancreas glands, (ii) protease from moulds, fungal origin which works in the pH range of 3.5- 5.0 referred to as an acid bate (iii) bacterial protease which work in the neutral pH range 6.2- 7.0 [7].

The present work deals with the application of the extracellular protease from *Bacillus cereus* MCM B-326. The efficiency was compared with that of the cattle dung and ComBate.

[II] MATERIALS AND METHODS

2.1. Organism and chemicals

A strain of *Bacillus cereus* MCM B-326 used was a buffalo hide isolate which had the ability to secrete protease. All chemical and media were purchase from Hi- Media Laboratories, Mumbai.

2.2. Enzyme preparation

The strain was maintained as a glycerol stock at -20°C. 2.8×10^8 cells of the organism *Bacillus cereus* MCM B-326 were inoculated into a medium containing 1% starch, 1% soybean meal, 0.3% CaCO₃ (pH 9.0). The flasks were kept under shaking conditions for 36 h at 30 °C. After 36 h the culture filtrate obtained was centrifuged at 13,000 g for 10 minutes to remove the biomass [8]. The supernatant was partially purified by ammonium sulphate precipitation (60% saturation) and the enzyme thus obtained was used for the evaluation of its activity on casein, azocoll and hide powder azure substrates and bating efficacy on chemically dehaired buffalo hide.

2.3. Enzyme assays

2.3.1. Caseinolytic assay

Protease activity was measured using caseinolytic assay [9]. The culture supernatant (1 mL) was incubated in 4 mL of 0.625% casein at 37 °C for 30 min. The reaction was stopped by 5 mL of trichloroacetic acid (5%) and

the casein hydrolysis product was measured by modified Folin Ciocalteu method [10], against inactive enzyme. A standard graph was generated using standard tyrosine of 10- 50 $\mu\text{g mL}^{-1}$. One unit of protease activity was defined as the amount of enzyme, which liberated 1 μg tyrosine per min at 37 °C.

2.3.2. Azocoll assay

Azocoll assay was determined using method described by Ensign & Wolfe [11]. Ten mg of azocoll was added to 2 mL of Tris-HCl buffer (pH 8.0); to it 0.5 mL of suitably diluted enzyme was added and incubated for 10 min at 37°C. The reaction mixture was centrifuged and the absorbance of the supernatant was measured at 580nm relative to a blank without enzyme. One unit of activity was defined, as the amount of enzyme required to increase the absorbance by 0.001 absorbance unit under assay conditions.

2.3.3. Hide powder azure (HPA) assay

Hide powder azure assay was determined using method described by Puvankrishnan & Dhar [7]. 25 mg of HPA substrate was incubated with different concentrations of enzyme (0.01, 0.02, 0.03 and 0.04 mL) at 37°C for 20 min. The mixture was centrifuged and the supernatant was read at 595nm. The graph was plotted for different enzyme concentrations and absorbance at 595nm. The slope was directly proportional to the enzyme activity.

2.4. Bating application

The bating action of the enzyme was evaluated on the laboratory scale. Three buffalo hide pieces (3 cm x 3 cm) were soaked in 300% (w/v) tap water; dehairing was done by traditional chemical- 10% lime and 2% sodium sulphide. The limed, experimental pieces were washed thoroughly and delimed with 150% water and 1% ammonium chloride for 40 min and then added bating agent- animal dung (1%), commercial bate (1%) and *B. cereus* protease (0.15%) separately. All the other operations were performed together [7].

2.5. Bating efficiency tests

For thumb impression test, the time taken by the bated pelt to regain its original shape after a thumb was pressed on the grain side, and the intensity of the impression was noted [5]. The scud (hair root, degraded protein. etc.) removal by scrapping with fingernails was assessed. The degree of slipperiness, cleanliness of the bated pelt pieces was categorized.

2.6. Histopathology of hides

Histopathology of cattle dung, enzymatically and commercial bate powder bated pelt were studied using a method described by John & Merrilline [12]. The hide pieces were dehydrated with 80, 95 and 100% (v/v) of alcohol gradients followed by xylene and then embedded in paraffin. The longitudinal sections of hide embedded in paraffin wax were obtained using microtome. The sections were fixed on slides using starch paste containing thymol, which acts as preservative. The sections were stained using Harris's haematoxylin stain followed by 0.5% (v/v) HCl and diluted ammonia. The slides were observed microscopically for opening up of collagen fibers.

[III] RESULTS AND DISCUSSION

The protease from *B. cereus* MCM B-326 was assessed for its potential use in bating step of leather processing. The specificity

of protease from *B. cereus*, ComBate and cattle dung with casein, azocoll and hide powder azure substrates is summarized in Table-1.

Table 1: Enzyme activities of different bating agents with different substrates

| Bating agents | Substrates and enzyme activity ($\text{Ug}^{-1}\text{min}^{-1}$) | | |
|--------------------------------|---|---------|-------|
| | Casein | Azocoll | HPA |
| Protease from <i>B. cereus</i> | 947.69 | 1935 | 310 |
| ComBate | 675.95 | 1180 | 243.3 |
| Cattle dung | 692.93 | 1725 | 153.3 |

HPA- Hide powder azure

From Table-1 it was observed that the ComBate and cattle dung have enzyme activities with casein, azocoll and hide powder azure, as substrates but it was less as compared with protease from *B. cereus*. Likewise hide powder azure and azocoll were evaluated for their susceptibility as collagen-rich substitutes for casein in assaying for proteolytic activity of bate [13]. Various proteolytic activities of bate were measured in drum liquor by Mozersky *et al.* [13-17]. Casein was a general protease substrate while azocoll and HPA were recommended substrates for elastase type of enzymes.

A qualitative assessment of the effect of the protease as a bating enzyme gave a highly slippery, silkier and clean pelts with a very fine grain texture. Scud loosening was very easy and the intensity of the thumb impression was very deep. Taking 22 seconds for treated with animal dung, 18 seconds for ComBate and 26 second for *B. cereus* protease to reshape after imprint. These tests give an indication of the extent of removal of the interfibrillary material that leads to better opening up of the fiber structure. Hameed *et al.* [5, 18] reported qualitative assessment of the effect of the crude protease from *B. subtilis* as a bating enzyme gave a slippery feel to the leather with a very fine texture of the grain. Scud loosening was very easy and the intensity of thumb impression was very deep taking 25 sec to reshape after imprint. Mozersky *et al.* [17] reported bating with a halophile protease active in 4M NaCl and found to yield leather with satisfactory physical characteristics. This high salt concentration will be used to loosen the tight bonding of decorin to collagen, thus rendering the proteoglycan more susceptible to proteolysis and removal from the hide.

The collagen fiber opening was confirmed by histological technique followed by microscopy. The microscopy of bated pelts with the bating agents is shown in Figure-1. This reveals a greater opening up of the fiber structure in the case of the pieces bated with *B. cereus* protease than with the cattle dung and ComBate. Collagen fibers were not damaged because of protease action and are shown in Figure-2.

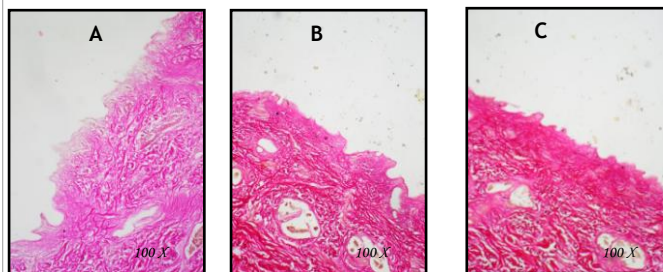


Fig: 1. Micrographs of pelt bated with A: animal dung, B: ComBate and C: protease from *Bacillus cereus* MCM B-326 (A and B showed disintegrated hair follicles, C showed empty follicles)



Fig: 2. Micrographs of pelts collagen bated with A: animal dung, B: ComBate and C: protease from *Bacillus cereus* MCM B-326 (A showed less opened collagen fibers, B showed moderate opened collagen fibers, C showed well-opened collagen fibers)

Scanning electronic microscopy of goat pelts bated with protease from *Streptomyces* sp. G₁₅₇ revealed a greater opening up of the fiber structure than the commercial enzyme bate [19]. Ding *et al.* [4] reported histological study of goatskin with pancreatin bates performing a function of removing epidermal matter, eliminating scud and cleaning grain surface. Zuo *et al.* [20] used surfactants for enhancing enzymatic bating of goat skin. Sirvaityte *et al.* [21] reported commercial enzymes LITHUDAC L and Novo Bate WB for bating of pelts after delimiting with peracetic acid. The results presented indicated that *Bacillus cereus* protease can work as a very good bating agent in leather processing.

[IV] CONCLUSIONS

The extracellular protease from *Bacillus cereus* MCM B-326 was found to be an effective bate as compared to cattle dung and ComBate.

FINANCIAL DISCLOSURE

The work was financially supported by NMITLI project on, "Biotechnology for leather- towards cleaner processing." sponsored by CSIR, Govt. of India

ACKNOWLEDGEMENT

Authors were greatly thankful to NMITLI project on biotechnology for leather- towards cleaner processing and Council of Scientific and Industrial Research (CSIR), New Delhi, India.

REFERENCES

- [1] Taylor MM, Bailey DG, Fearheller SH. [1987] A review of the uses of enzymes in the tannery. *J Am Leath Chem Assoc* 82: 153–165.
- [2] Purushotham H, Malathi S, Rao PV, Rai CL, Immanuel M.M, Raghavan KV. [1996] Dehairing enzyme by solid-state fermentation. *J Soc Leath Technol Chem* 80: 52–56.
- [3] Thanikaivelan P, Rao JR, Nair BU, Ramasami T. [2004] Progress and recent trends in biotechnological methods for leather processing. *Trend Biotechnol* 22: 181– 188.
- [4] Ding H, Sun L, Liang C. [2005] Action of pancreatin on residual epidermis of goatskin– examination via histological changes during bating. *J Soc Leath Technol Chem* 89: 141– 144.
- [5] Hameed A, Natt MA, Evans CS. [1996] Production of alkaline protease by a new *Bacillus subtilis* isolate for use as a bating enzyme in leather treatment. *World J Microbiol Biotechnol* 12: 289– 291.
- [6] Puvankrishnan R, Dhar SC. [1986] Recent advances in the enzymatic depilation of hides and skins. *Leath Sci* 33: 177–191.
- [7] Puvankrishnan R, Dhar SC. [1988] Enzyme technology in beamhouse practice. Central Leather Research Institute, Adyar, Chennai, 164–165.
- [8] Nilegaonkar SS, Zambare VP, Kanekar PP, Dhakephalkar PK, Sarnaik SS. [2007] Production and partial characterization of dehairing protease from *Bacillus cereus* MCM B– 326. *Biores Technol* 98: 1238–1245.
- [9] Kanekar PP, Nilegaonkar SS, Sarnaik SS, Kelkar AS. [2002] Optimization of protease activity of alkaliphilic bacteria isolated from an alkaline lake in India. *Biores Technol* 85: 87– 93.
- [10] Lowry OH, Rosebrough NJ, Farr AL, Randall RJ. [1951] Protein measurements with Folin phenol reagent. *J Biol Chem* 193: 265–275.
- [11] Eising JC, Wolfe RS. [1965] Lysis of bacterial cell walls by an enzyme isolated from a *Myxobacter*. *J Bacteriol* 90: 395–402.
- [12] John DB, Merriline J. [2002] Theory and practice of histopathological techniques. 5th edition. Churchill publishing company.
- [13] Mozersky SM, Bailey DG. [1992] Hide powder azure and azocoll as substrates for assay of the proteolytic activity of bate. *J Am Leath Chem Assoc* 87: 287–295.
- [14] Mozersky SM, Baynes MA, Bailey DG. [1993] Measurement of the proteolytic activity of bate in drum liquor. *J Am Leath Chem Assoc* 88: 283–290.
- [15] Mozersky SM, Baynes MA and Bailey DG. [1995] Optimization of the assay of bate and drum liquor for proteolytic activity. *J Am Leath Chem Assoc* 90: 235–242.
- [16] Mozersky SM, Deiss J, Bailey DG. [1999] Viscometric assays of the protease activity of bate and drum liquor. *J Am Leath Chem Assoc* 94: 51–59.

- [17] Mozersky SM, Allen OD, Marmer WN. [2002] Vigorous proteolysis: reliming in the presence of alkaline protease and bating (post- liming) with an extremophile protease. *J Am Leath Chem Assoc* 97: 150–156.
- [18] Hameed A, Natt MA, Evans CS. [1996] Comparative studies of a new microbial bate and the commercial bate ‘Oropon’ in leather treatment. *J Ind Microbiol* 17: 77–79.
- [19] Padmavathi S, Chandrababu NK, Chitra S, Chandrakasan G. [1995] Application of the extracellular protease from the culture filtrate of *Streptomyces* spp. G₁₅₇ in bating. *J Soc Leath Technol Chem* 79: 88– 90.
- [20] Zuo Q, Chen W, Hlavacek P. [2009] Effect of surfactant on enzyme and skin in bating process. *XXX congresso IULTCS, Beijing, 2–27*: pp 1–6.
- [21] Sirvaityte J, Valeika V, Beleska K, Valeikiene V. [2006] Bating of pelts after deliming with peracetic acid. *Proc Estonian Acad Sci Chem* 55: 93–100.

ABOUT AUTHORS



Dr. Vasudeo Zambare, MSc, PhD, FISBT, is Research Scientist in the Center for Bioprocessing Research & Development, South Dakota School of Mines & Technology, USA. Dr. Vasudeo specializes in microbial enzymes, extremophiles, renewable energy (biomass, biofuels and bioenergy), antimicrobial peptides and biodegradable plastic for biomedical applications. In his research career, he published research articles (>20), book chapters (2), abstracts in conferences (>35), patents filed (3). Recently, he is honoring as associate editor, technical editor, advisory board member and editorial board member for more than 32 International research journals and as reviewer for more than 52 international journals.



Dr. Smita Nilegaonkar, MSc, PhD, FISBT, has been working as Scientist D, in MACS-Agharkar Research Institute, Pune, M.S. India. Working in field of biotechnology, especially in microbial production of industrially important compounds, enzymes & their inhibitors, development processes for enrichment of functional foods. She is a current Fellow-member of the International Society of Biotechnology (India). Research Publications > 25, Chapters 2, Books 1, Patents Indian - one sealed two filed, patent -US/German filed one.



Dr. Pradnya Kanekar, MSc, PhD, has been working as a scientist G and Head, Microbial Sciences Division of MACS-Agharkar Research Institute, Pune, M.S., India. She has post-doctoral research experience of 30 years since 1980. Her main areas of interest are 1. Biodegradation and bioremediation of toxic organic pollutants, 2. Microbial diversity and conservation of bacteria and archaea, 3. Biotechnological potential of extremophiles. So far 12 students have been awarded Ph.D. degree in the subject of Microbiology of Pune University and six students are registered for Ph.D. degree, 51 papers are published in peer reviewed journals, 4 Indian patents are granted, 3 patents applied and one technology transferred for commercialization.

RESEARCH: BIOINFORMATICS

MULTIFRACTAL ANALYSIS OF PROTEIN AGGREGATES TO DERIVE PROTEIN-SPECIFIC SIGNATURE

Hrishikesh Mishra, Tapobrata Lahiri*

Division of applied sciences and Indo-Russian center for biotechnology, Indian Institute of Information Technology, Allahabad-211012, INDIA

Received on: 3rd-Aug-2010; Revised on: 13th-Oct-2010; Accepted on: 19th-Oct-2010; Published on: 15th-Nov-2010.

*Corresponding author: Email: tlahiri@iiita.ac.in Tel: +91-5322922229; Fax: +91-5322430006

ABSTRACT

Deriving a property of a protein that is unique to it has well known significance since the study on ab initio model based derivation of protein structure where uniqueness of protein sequence is taken as the source of specificity of protein structure. In this direction, Heat denatured protein aggregates (HDPAs) of proteins were studied with an objective to derive some multi-fractal markers specific to constituent protein that may be further utilized to extract information of the seed protein. Since Ordinary microscopic images of aggregates were analyzed to extract Intensity Level-based Multifractal Dimension (ILMFD) features. ILMFD features include four different features, perimeter fractal dimension (ILMFD_P), perimeter-area relationship (ILMFD_{PAR}), Area fractal dimension (ILMFD_A) and Perimeter-area fractal dimension (ILMFD_{PA}) that were calculated using fractal computations considering perimeter, and area of aggregate images. Feed forward backpropagation network was used to classify the proteins using different ILMFD parameters. It was found that ILMFD features could discriminate the proteins used in our study, that points to their potential to serve as unique property or marker of a protein. Further to validate the results, the outputs from ANN were clustered, and the outputs clustered in the largest cluster were found to significantly improve the result in class decision given by ANN.

Keywords: Heat denatured protein aggregate; Multifractal dimension; Protein-marker; clustering

[1] INTRODUCTION

Protein aggregation has been considered as an unwanted and unproductive phenomenon in biological applications involving proteins [1]. It can be defined as a process by which a homogeneous protein solution separates into two phases comprising aggregate phase having significant intermolecular interactions and the other one having dilute supernatant of isolated protein [2]. generally accompanied by conformational change of protein, which can be induced by thermal, enzymatic or chemical perturbations affecting the native folded structure of protein [3]. But recently several studies have pointed towards specificity of aggregates to their seed proteins.

Bohr et al (1997) [4]. through their experiment on native protein aggregate by electronic, atomic force and ordinary microscope, have shown that the structure of aggregates of proteins are strongly influenced by shape of constituent individual protein molecules. Also, from the study done by Taubes we find that protein aggregates are not as nonspecific as earlier believed [5].

In a simulation study on protein aggregation, Patro and Przybycien showed that variation in monomer surface property significantly affects the structure of kinetically irreversible protein aggregates [6]. Another study indicated that aggregation properties are affected by structural changes in proteins. Change in protein structure is found to significantly affect the topology and energetics of contacts within aggregates and thermodynamic drive towards aggregation [7].

Recently it has been found that aggregation is a generic property of polypeptide chains and aggregation propensity differs with difference in structure and environment [8]. Some studies have shown that a minor change in amino acid sequence of protein can prevent or increase aggregation of protein. In a study done on viral coat proteins, King et al., found that mutant viral coat protein having a single amino acid change, folded at low temperatures normally, but at higher temperatures it self-assembled into aggregates. This aggregation at high temperatures was not found in normal protein [5]. Another study done by David Brems et al., on bovine growth hormone,

showed that mutation prevented its aggregation but did not affect its folding [9]. These studies indicate that aggregation may be preprogrammed into amino acid sequence just like folding and aggregates should not be considered as just a nonspecific mess.

Taking cue from these studies, we have been searching towards a suitable aggregate feature that can be used as a marker showing specificity of aggregates to individual proteins. The background behind this effort is the expectation that such unique aggregate based feature should be map-able to individual protein property, especially structural property. Like the structural information we draw from protein crystal which is eventually an ordered assembly of protein and mostly scarce, we want to draw structural information of protein from its aggregate which is apparently not so ordered but available for almost all the proteins. To accomplish this goal, in this work we have extracted a scale and rotation independent feature Intensity Level-based Multifractal Dimension (ILMFD), based on mass fractal dimension of aggregates to study the rough pattern of heat denatured aggregates [10, 11]. As ILMFD is basically an aggregate-image based feature, it is quite likely that it captures the rough shape and texture of 3D-aggregates in its 2D-projected form. In current work, we have extracted three more features, to be included in ILMFD feature set and utilized them in a novel neuro-clustering classifier. This new approach has shown promise to significantly increase the specificity of ILMFD feature set to individual protein.

[II] MATERIALS AND METHODS

2.1. Formation of protein aggregates

The proteins used were Albumin, Cytochrome c, Ferritin, Hemoglobin, Insulin and Lysozyme. Proteins were purchased from Sigma Aldrich Inc. (USA). Water used in the experiments was purified by Millipore Water System (Model: Millipore, USA). Each Protein was dissolved in Millipore water at concentration of 25 mg/cc and kept at 100°C for 15 minutes to obtain its Heat Denatured Protein Aggregates (HDPAs).

2.2. Procuring microscopic images of aggregates

Suspension having homogeneously distributed HDPAs was spread over Hemocytometer slides (Model: Neubauer Chamber, Marienfeld, Germany) and visualized under phase contrast mode of compound light microscope (Leica Model DML-B2) at 400× magnification. Images of aggregates were captured using a digital camera (Canon PowerShot S50) attached with the microscope, at 2× optical zoom, resulting in to total magnification factor of 800×. For each protein 50 images of HDPAs at different fields of views were captured to create an aggregate image dataset.

2.3. Preprocessing and intensity plane slicing of images

Each aggregate image was converted to grey scale and resized to 1/3rd of the original size 2592x1944 pixels, to reduce computational complexity. Background of each aggregate image was made black using

Adobe Photoshop 7.0 to nullify the effect of background on ILMFD parameters calculated from images. Each image, was split into 10 binary images on the basis of fixed intensity-ranges by applying the rule that in a binary image representing an intensity range, only the pixels having intensity values falling in that intensity range, would be kept as 1, while all other pixels would be assigned a value of zero. Computationally, intensity interval between maximum and minimum intensity of a particular image was divided into 10 smaller and equal intervals or ranges.

2.4. Deriving ILMFD features from aggregate images

Area (A), perimeter (P) of aggregates for 10 binary images representing each aggregate image were calculated at different scales of measurement (S) using box counting method. Four types of ILMFD features were derived using Area, and perimeter calculated at different scales of measurement i.e., box size [12,13]. Area (A) was calculated as number of boxes covering the aggregate in the image. Similarly, perimeter (P) was measured as the number of boxes making the periphery of the aggregate in the image. Perimeter fractal dimension was calculated as the slope of the linear regression plot between log(P) and log(S). Perimeter-area relationship was calculated as slope of linear regression plot between log(P) and log(A) at different box sizes (S). Area fractal dimension was calculated as the slope of linear regression plot between measured log(A) and log(S). Similarly perimeter-area fractal dimension was calculated as linear regression plot between two variables x, and y where $x = \log(P/S)$, and $y = (\log(A))/2 - \log(S)$ [14]. Thus each aggregate image was represented by 10 fractal dimensions (one for each binary image), cumulatively referred to as ILMFD where, D_i is fractal dimension of one intensity level:

$$D = \{D_i\}_{i=1}^{10}$$

Thus we derived four different types of ILMFD parameters as ILMFD_A, ILMFD_P, ILMFD_{PA}, and ILMFD_{PAR} from area fractal dimension, perimeter fractal dimension, perimeter area fractal dimension and perimeter area relationship respectively.

2.5. Classification by ILMFD parameters using artificial neural network

Each of the four ILMFD features was used separately for classification of images into different classes based on their constituent protein. The classification decisions from different ILMFD features were obtained using feed forward backpropagation networks where normalized values of ILMFD features I_F was used as input vector. ILMFD data set obtained from 300 images of all proteins, was divided in to training and test sets, by randomly picking data for 210 images as training set and for remaining 90 images as test set. Such five training and test sets were chosen randomly for training and testing the neural network based classifier. Each training and test ILMFD data was normalized by subtracting their column mean calculated from respective training ILMFD data.

Same network architecture was used for all the four ILMFD features. It consisted of one hidden layer apart from input and output layers. While the input layer comprised of 10 neurons, hidden layer consisted of 8 nodes. Output layer had six neurons to represent six classes of our interest. Tan sigmoid transfer function was used in hidden and output layers. Mean square error was used as performance function. Trained networks were simulated with normalized test ILMFD feature data for validation.

2.6. Classification by ILMFD parameters using neuro-clustering classifier

Classification decisions obtained for test sets of each protein were clustered using k means clustering. Value of k was kept as 2, considering possibility of two types of decisions i.e., correct or incorrect. Centre of the decisions grouped in larger cluster were matched with correct decisions of test dataset to validate the decision tendency of trained networks.

[III] RESULTS AND DISCUSSION

3.1. Potential of ILMFD features to classify and recognize individual proteins

The neural networks trained with different ILMFD features, were simulated for their respective test sets. To remove the possibility of any bias, training and testing of neural networks, was done using five different randomly chosen training and test sets from whole data. Results for neural networks giving maximum efficiency of protein classification on test sets as well as average efficiency of all networks for each ILMFD feature are shown in table 1. Maximum efficiency of protein classification on test set was found for features ILMFD_P and ILMFD_{PAR}. Similarly network-average of efficiencies of five networks for classification of proteins using these same features were found to be the maximum among the features selected in our study [Table-1].

Protein-wise sensitivity and specificity of classification using neural networks giving maximum efficiency on test set are given in Table-2. In Table-3, the efficiency in classifying a protein using decision clustering model of neural network outputs (we referred as neuro-clustering) has been shown.

| ILMFD Feature | Training Set | | Test Set | |
|----------------------|---|-------------------------------------|---|-------------------------------------|
| | Efficiency of network giving Maximum Efficiency on test set | Average Efficiency of five networks | Efficiency of network giving Maximum Efficiency on test set | Average Efficiency of five networks |
| ILMFD _A | 93.81 | 94.57 ± 0.87 | 74.44 | 70.44 ± 3.20 |
| ILMFD _P | 98.57 | 94 ± 6.96 | 80 | 76.88 ± 2.65 |
| ILMFD _{PA} | 96.67 | 94.95 ± 1.37 | 67.78 | 63.11 ± 3.08 |
| ILMFD _{PAR} | 94.76 | 94.85 ± 2.90 | 80 | 75.78 ± 2.53 |

Table: 1. Results of classification in percentage for proteins using different ILMFD features of HDPAs

| Class | ILMFD _A | | ILMFD _P | | ILMFD _{PA} | | ILMFD _{PAR} | |
|--------------|--------------------|-------|--------------------|-------|---------------------|-------|----------------------|-------|
| | Sens | Spec | Sens | Spec | Sens | Spec | Sens | Spec |
| Albumin | 61.54 | 76.62 | 57.14 | 84.21 | 63.64 | 68.35 | 90 | 78.75 |
| Cytochrome c | 64.71 | 76.71 | 80 | 80 | 37.5 | 74.32 | 63.16 | 84.51 |
| Ferritin | 73.68 | 74.65 | 100 | 75.34 | 78.57 | 65.79 | 100 | 76 |
| Hemoglobin | 83.33 | 72.22 | 94.12 | 76.71 | 81.25 | 64.86 | 93.33 | 77.33 |
| Insulin | 100 | 70.13 | 92.86 | 77.63 | 83.33 | 63.89 | 82.35 | 79.45 |
| Lysozyme | 60 | 76.25 | 46.15 | 85.71 | 60 | 69.33 | 57.14 | 84.21 |

Table: 2. Results of neural network based classification in percentage for each protein based on four different ILMFD features: 'Sens' and 'Spec' represent sensitivity and specificity respectively

| | ILMFD _A | ILMFD _P | ILMFD _{PA} | ILMFD _{PAR} |
|------------|--------------------|--------------------|---------------------|----------------------|
| Efficiency | 100 | 100 | 67 | 100 |

Table: 3. Results of percentage efficiency for neuro-clustering based classification for each protein based on four different ILMFD features

Efficiency of ILMFD parameters to classify proteins is indicative to their potential to recognize and discriminate each of the proteins and thus to serve as markers for each proteins.

For this reason we present efficiency-profile of different ILMFD features in Tables-1, -2 and -3.

3.2. Selection of protein aggregates as study material

The idea behind this work originated from various studies on protein aggregates, indicating the specificity of aggregate properties to their constituent proteins. On the other hand limited applicability of experimental methods like x-ray crystallography, NMR, prediction methods like homology modeling and threading for protein structure determination etc. predicated the need for search of novel methods for determination of protein structure and structure based features. Easy availability of protein aggregates through simpler experimental set up as compared to protein crystals, encouraged us to investigate the possibility of deriving some protein specific aggregate features, which would be protein specific and could be further used to map some functionally important structure features like protein functional sites.

3.3. Suitability of aggregate data representation

An aggregate image represents the natural three dimensional texture of aggregate in two dimensional forms [15, 16]. Each image was sliced into different intensity planes using gray level intensity based method into binary images where each intensity level was supposed to grossly capture the three dimensional depth of the aggregate. At each intensity level four types of fractal dimensions were calculated. The whole set of fractal dimensions calculated from all the intensity planes constitute the multi-fractal features for a particular aggregate image. As we had considered area, and perimeter measurements at different scales of measurement, it is quite likely that information on geometrical rough-pattern of aggregate surface and perimeter was suitably represented through these multi-fractal dimension features. ILMFD feature set tries to capture the roughness pattern of aggregates at surface and peripheral parts, which may be specific to the aggregates of particular protein. Thus ILMFD features have potential to be used as a protein specific aggregate feature.

3.4. Robustness of ILMFD Features

The probable reason behind the high efficiency obtained through ILMFD features may be suitable representation of possibly unique patterns of aggregate surface and perimeter using ILMFD features. ILMFD features capture aggregate surface and perimeter patterns hidden in various intensity-depths. Moreover, the number of intensity levels was fixed after several trials, to get sufficient and equitable representation of intensity depths. Further studies may be done to find an optimum number of intensity levels to represent various intensity depths in aggregate images more reasonably.

3.5. Applicability of ILMFD features

The work dealt with development of a new approach for deriving structural information of protein by using light-microscopic images of protein aggregates as input data that is subsequently processed and mined for this purpose. The objective of ILMFD based classification of protein was to find a set of features which will serve as unique structural or functional signature. As aggregation is generally driven by interaction of its constituent proteins it is interesting to see whether this interaction has specificity to the structure or function of its ingredient i.e., individual protein. The proteins chosen by us have diverse function and patho-physiological behavior. Therefore a specific pattern of these proteins was expected from their aggregates. The capability of ILMFD features towards this direction to discriminate the proteins selected for this study is quite encouraging. For enhancing the discriminatory (i.e., classifying) power a novel neuro-clustering approach was adopted in which the overall efficiency of classification was found to increase significantly. Moreover, our approach utilizes a very simple protocol based on computation of data obtained from heat-denaturation of protein and ordinary microscopy. Therefore it is worth investigation to see whether this protocol may be utilized as a tool to identify proteins on the basis of their structural or functional families without taking the help of their PDB structures.

3.6. Applicability of neuro-clustering classifier

Concept of neuro-clustering classifier was introduced taking cue from the decision making process of human brain. Notion of group decision was applied using multiple instead of a single test data. In most cases larger cluster of decisions was found to represent the general tendency of decisions, while the smaller cluster was found to represent noise. Centre of larger cluster was found to be a close approximation of correct class decision in majority of cases leading to significant improvement in classification efficiency for all the ILMFD features except ILMFD_{PA} [Table-3]. This kind of approach may find its applications in various other classification problems dealing with biological data.

[V] CONCLUSION

Promising results obtained from this study show the specificity of aggregate properties to constituent proteins. In the context of limited applicability of conventional complex methods for protein structure determination like x-ray crystallography and NMR, aggregation based methods hold potential to serve as starting point for development of novel alternative methods for derivation of protein structural features. Further exploration is required in this direction to develop methods to utilize these aggregate features to derive functionally important structural feature of protein like functional sites which lie on surface.

Moreover the concept of neuro-clustering introduced in this work proved to be a very useful classifier to handle complexity in input test dataset which points possible scope of its applications in other biological classification problems also.

FINANCIAL DISCLOSURE

This work was financially supported by the Ministry of Human Resource Development, Govt. of India (grant no.F.26-14/2003.T.S.V.Dated 14.01.2004) and the Indian Council of Medical Research, Government of India (grant no. 52/8/2005-BMS dated 04.02.2010).

ACKNOWLEDGEMENT

We acknowledge helpful discussion with Prof. Harish Karnik, Department of Computer Science & Engineering, Indian Institute of Technology, Kanpur, India.

REFERENCES

- [1] Okanojo M, Shiraki K, Kudou M, et al. [2005] Diamines prevent thermal aggregation and inactivation of lysozyme. *J Biosci Bioeng* 100: 56–561.
- [2] Pappu RV, Wang X, Vitalis A, et al. [2008] A polymer physics perspective on driving forces and mechanisms for protein aggregation. *Arch Biochem Biophys* 469:132–141.
- [3] Weijers M, Barneveld PA, Stuart MAC, et al. [2003] Heat-induced denaturation and aggregation of ovalbumin at neutral pH described by irreversible first-order kinetics. *Protein Sci* 12:2693–2703.
- [4] Bohr H, Kühle A, Sørensen AH, et al. [1997] Hierarchical organization in aggregates of protein molecules. *Z Phys D* 40:513–515.
- [5] Taubes G. [1996] Misfolding the Way to Disease. *Science* 271:1493–1495.
- [6] Patro SY, Przybycien TM. [1994] Simulations of Kinetically Irreversible Protein Aggregate Structure. *Biophys J* 66:1274–1289.
- [7] Pullara F, Emanuele A, Palma-Vittorelli MB, et al. [2007] Protein aggregation/crystallization and minor structural changes: universal versus specific aspects. *Biophys J* 93:3271–3278.
- [8] Monsellier E, Ramazzotti M, Taddei N, et al. [2008] Aggregation propensity of the human proteome. *PLoS Comput Biol* 4:e1000199.
- [9] Brems DN, Plaisted SM, Havel HA, et al. [1988] Stabilization of an associated folding intermediate of bovine growth hormone by site-directed mutagenesis. *Proc Natl Acad Sci USA* 85:3367–3371.
- [10] Lahiri T, Mishra H, Sarkar S, et al. [2008] Surface characterization of proteins using Multifractal property of heat-denatured aggregates. *Bioinformation* 2:379–383.
- [11] Lahiri T, Mishra H, Kumar U, et al. [2009] Derivation of a protein-marker from heat-denatured protein-aggregate. *Online J Bioinformatics* 10:29–39.
- [12] Kawaguchi E, Taniguchi R. [1989] The depth first picture-expression as an image thresholding strategy. *IEEE T Syst Man Cyb* 19:1321–1328.
- [13] Zmeškal O, Veselý M, Nežádal M, et al. [2001] Fractal Analysis of Image Structures. *HarFA e-journal* 1:3–5.
- [14] Feder J. [1989] *Fractals*, Plenum Press, New York, USA.
- [15] Tuceryan M, Jain AK. [1998] Texture Analysis, in: *The Handbook of Pattern Recognition and Computer Vision*, Chen CH, Pau LF, Wang, PSP., (eds) World Scientific Publishing Co., Hackensack, New Jersey, USA, p. 207–248
- [16] Haralick M. [1979]. Statistical and Structural Approaches to Texture, *Proc IEEE* 67:786–804.

ABOUT AUTHORS



Mr. Hrishikesh Mishra received M.Tech. degree in bioinformatics from Indian Institute of Information Technology, Allahabad, India. He is currently a Ph.D. scholar in bioinformatics at Indian Institute of Information Technology, Allahabad, India, under guidance of Dr. Tapabrata Lahiri. His research interests include artificial intelligence and computational biology. He has authored 6 publications.



Dr. Tapabrata Lahiri is Associate Professor and Head of the Division of Applied Sciences and Indo-Russian center for Biotechnology at Indian Institute of Information Technology, Allahabad, India. His research interests include artificial intelligence and biophysics. He has 36 publications in this credit.

COMMENTARY: NEUROSCIENCE

NEUROAIDS: A REAL CONCERN

Ashish Swarup Verma*, Udai Pratap Singh, and Anchal Singh

*Amity Institute of Biotechnology, Amity University Uttar Pradesh, Sector-125, NOIDA (UP)-201303, INDIA*Received on: 11th-Aug-2010; Revised on: 9th-Nov-2010; Accepted on: 12th-Nov-2010; Published on: 2nd-Dec-2010.*Corresponding author: Email: asverma@amity.edu, ashish-gyanpur@hotmail.com Tel: +91-120-4392757; Fax: +91-120-4392295**ABSTRACT**

Improved antiretroviral treatments are still unable to cure HIV infections, therefore chronically low levels of HIV replication continues in patients. Long-term low replication of HIV leads to accumulation of virotoxins, which could be a reason for neurotoxicity in long-term HIV survivors. Nowadays, more than 50% of HIV patients are presented with neuropsychiatric complications, known as NeuroAIDS. Increase in life-span of HIV seropositives, along with addition of new infections every year is a real concern for NeuroAIDS as a new and emerging health problem.

Keywords: NeuroAIDS; neuropsychiatric disorder; HIV; ART; BBB**COMMENTARY**

Some of the common neuropsychiatric diseases are mood disorders, schizophrenia, addiction, dementia, epilepsy, etc. Usually, a combination of neurological and psychiatric disorders is categorized under neuropsychiatric disorders, which contribute ~15% of world's disease burden [1]. In the recent past, various neuropsychiatric complications have been reported among human immunodeficiency virus (HIV) seropositive individuals with much higher frequencies than their normal occurrence in uninfected population. Neuropsychiatric complications among AIDS patients are collectively called as NeuroAIDS. Some of the most common neuropsychiatric complications among HIV seropositives are HIV-associated dementia (HAD), HIV-associated encephalopathy (HIVE), HIV-associated minor cognitive/motor disorder (MCMD), etc. It has been estimated that >50% HIV seropositives show signs and symptoms of neuroAIDS at later stages of HIV infection [2].

In 1981, the first report of HIV infection came from Los Angeles, USA, where five gay men were infected with *Pneumocystis carinii* pneumonia (PCP) [3]. At that time, neither the HIV nor the AIDS terms were in use in medical dictionary. The AIDS name was adopted for this disease by Center for Disease Control and Prevention (CDC), Atlanta, USA, in 1982. The causative organism for death of these gay men was discovered by Luc Montagnier (France) in 1983 and

confirmed by Robert Gallo (USA) in 1984. Both of them proposed different names for the same virus and those names were Lymphadenopathy-Associated Virus (LAV) and Human T-cell Lymphotropic Virus (HTLV), respectively. But the final name was coined as HIV in 1986 by the International Committee on Taxonomy of Viruses. Soon, reports of HIV infections started pouring in from all over the world. Explosion in the number of HIV-infected patients gave a sense of an epidemic, and HIV was widely spreading without any limitations of physical boundaries. No one was immune to HIV infections; HIV was known to infect men, women, children and even newly born babies alike. People from all age groups, ethnicity and nationality are known to be victims of HIV infections. Spread of HIV infections has been brought under control to a great extent by now; still, it is spreading and affecting various communities. The impact of HIV infection to certain communities e.g., African countries has been devastating [4].

Statistics about HIV infections, prevalence and progression towards AIDS are still shocking. As per new estimates by UNAIDS (2009), >34 million HIV-infected people are living in the world, out of which >2 million HIV infection cases are diagnosed in children below the age of 15 years. Although various effective measures are taken to control the spread of HIV, it is still an astonishing fact that according to UNAIDS

report >2 million people get new HIV infection every year [Table-1]. Additions of such high numbers of new infections are still making this situation worse day-by-day. These numbers do not give any jitter, if calculated as percentage of total world population, which turns out to be <0.5% of total

human population. But the absolute numbers of 34 million infected people along with addition of 2.4 million new infections every year is a serious and real concern for a chronic and fatal disease like AIDS [5].

Table: 1. HIV/AIDS epidemic till 2008: At Glance*

| | Living with HIV | New Infection [†] | Death [†] |
|--------------|-----------------|----------------------------|--------------------|
| | ← | (in millions) | → |
| Men | 15.70 | 1.15 | 0.85 |
| Women | 15.70 | 1.15 | 0.85 |
| Children | 02.00 | 0.43 | 0.28 |
| Total | 33.40 | 2.73 | 1.98 |

*, Adapted from UNAIDS Report, 2009. †; Annual estimate

AIDS is the final stage preceded with HIV infections, which finally leads to the death of patients. Initially, a high incidence of mortality was reported among HIV seropositives, as there was no medicine available for HIV control. Later, azidothymidine (AZT), an antiretroviral drug became the 1st available treatment for HIV infections. Since then, HIV medications have achieved marked improvements in their efficacy, which helped to reduce morbidity and to increase survival among HIV seropositives. Undoubtedly, antiretroviral drugs have added millions of life years among HIV seropositives, when the data is compounded. Nonetheless, HIV infections can only be controlled and cannot be cured, which simply translates into the fact that if someone is infected with HIV, that person has to live with it life-long and wait for its progression towards full blown AIDS, that will bring an end to his/her painful existence. Certainly, improved medications have significantly delayed the onset of AIDS. The new treatment regimens like highly active antiretroviral treatments (HAART) have significantly contributed towards delay in the onset of AIDS. At present, all the available HIV treatments are far from perfect, because each and every medication and treatment regimen have their own limitations and side effects.

In fact, the benefits and drawbacks of HIV medication represent the two sides of the same coin. On the one side, anti-HIV drugs have enhanced the survivability among HIV seropositives, while on the flip side these drugs have indirectly contributed towards the appearance of various neuropsychiatric complications among these patients. Specifically, longer survival with chronic infections like HIV causes decrease in immune-competency of the host, which in turn increases the probability to be infected with different opportunistic infections like PCP, pneumonia, Kaposi's sarcoma, *etc.* Still, if we take a closer look at initial findings of HIV cases, signs and symptoms of neuropsychiatric disorders are not new. Unfortunately, even initial cases of AIDS had been reported with neuropsychiatric signs and symptoms, but

failed to attract a significant level of attention, because at that point of time, priority was given to control HIV infections, and efforts were directed to develop strategies to prevent its spread. At present, better access of antiretroviral drugs to HIV patients have extended their life; as a result HIV seropositives live longer, but they now face NeuroAIDS a new complication associated with HIV infections, as a consequence of their longer survival.

According to some estimates, >50% long-term HIV seropositives show signs and symptoms of NeuroAIDS. With this high prevalence of NeuroAIDS, in the near future, we expect that a huge number of HIV patients will be living with NeuroAIDS worldwide. Therefore, the burden of NeuroAIDS to society is expected to rise as days pass by [Table-2]. This fact can be simply understood from the UNAIDS (2009) report, which informs that everyday ~7400 people get infected with HIV, while ~5500 die with AIDS. In other words, every day we are adding ~1900 patients, which translates into ~0.7 million HIV infected individuals annually.

NeuroAIDS should be considered as a significant health issue due to variety of reasons: 1) the number of patients is ever increasing on daily basis, 2) symptoms of NeuroAIDS hit almost at the prime of age of a human being, *i.e.* between the age of ~35-45 years, 3) high costs for continuous supply of antiretroviral medications, 4) NeuroAIDS patients need additional medication, 5) usually, NeuroAIDS symptoms render these patients least productive in their life resulting in substantial loss of their individual or family income, and 6) need for a care-taker or care-giver, which again financially translates into extra loss of income due to active involvement of another family member, who will assume the role of a care-giver, or a possibility of extra expenditure to be incurred to the family for the health care of a NeuroAIDS patient, if they hire a professional care-giver. These are some compelling reasons

to realize the importance and adverse impact of NeuroAIDS on society [6].

Pathophysiologically, NeuroAIDS is a result of either direct HIV infection to CNS/brain or induction of neurotoxicity, as a consequence of HIV infections. An HIV infection to brain is an intriguing phenomenon for clinicians as well as for biomedical scientists. CNS/brain is the most protected organ system of body, as it is separated from rest of the body by blood brain barrier (BBB). Even with the presence of protective barrier to brain, some evidence for HIV infection to brain was reported from cadaver cases of HIV/AIDS patients. Still, it is difficult to explain HIV infection to brain, as the majority of brain cells are not readily infected by HIV. Some of the most common cells present in CNS are astrocytes, oligodendrocytes, microglia, perivascular macrophages and neurons. So far, neurons have been shown to be non-permissive to HIV infection, which is understandable, because they do not express the primary receptors used by HIV, *i.e.*,

CD4 [7]. Microglia and perivascular macrophages express CD4 receptors on their cell surface. However, rather than loss of microglia and perivascular macrophages due to HIV infections, neuronal loss has commonly been observed in cases of NeuroAIDS. Important co-receptors like CXCR4 and CCR5 are under active search for their role in HIV infections to the brain. At present, it seems like NeuroAIDS is more of a result of neurotoxicity rather than HIV infections. This neurotoxicity may play a vital role in neuronal loss, although the triggers of neurotoxicity are currently unknown. Collectively, several issues have been raised that are under active consideration, such as: 1) Is HIV itself responsible for NeuroAIDS? 2) Is NeuroAIDS a secondary complication emerged due to long-term antiretroviral treatment (ART)? 3) Low or negligible penetrance of ART in brain. 4) Are low levels of persistent and chronic HIV infection contributing towards development of NeuroAIDS? or 5) Is it a combined effect of all these possibilities? The present understanding of NeuroAIDS and its causes remain still unclear [8].

Table: 2. Predication for expected numbers for NeuroAIDS*

| | Living (in millions) | Expected Rise [†] (in %) |
|----------|-------------------------|--------------------------------------|
| Men | 07.80 | 15 |
| Women | 07.85 | 15 |
| Children | 01.00 | 7.5 |

*; Prediction based on the assumption that all HIV seropositives (including new infections) have access to antiretroviral treatment and maintain a reasonable healthy state. †; Annual estimate

A low level of HIV replication continues even when HIV is below detection levels in patients, which can cause chronic accumulation of different virotoxins and cytokines (pro-inflammatory and inflammatory). These biomolecules get accumulated in circulation and may alter physiology of BBB, which may support entry of these molecules as well as HIV along with T-cells and monocytes (infected) present in peripheral circulation. Certainly, it is due to breach in the most protective layer, *i.e.* BBB. It seems like neurons are most vulnerable to any of these physiological/pathological alterations in brain and they respond to these changes by neuronal death. Recovery of neuronal loss is impossible due to the inherent characteristics of neurons, *i.e.* their inability to regenerate. On the other hand, microglia and perivascular macrophages are the only cells that are positive for primary receptors for HIV infection, *i.e.* CD4, and they serve as a reservoir for HIV infection by remaining latently infected for a longer time, or they retain undetectable levels of HIV replication. But at some point in time, HIV replication may get triggered in these cells and they become the major source of HIV replication in brain, although the nature of that trigger, is still a question for scientific discovery and debate. A low level

of HIV replication in microglia and perivascular macrophages is considered as one of the major reason for neurotoxicity, which ultimately leads to neuronal loss as a major pathological phenomenon for NeuroAIDS. While at late stages of HIV infection, active replication of HIV in these cells could accelerate progression of NeuroAIDS. Therefore, there are various underlying mechanisms at cellular and molecular levels to induce, maintain and worsen NeuroAIDS. This warrants a need for additional thorough studies on the mechanisms of NeuroAIDS, so that this problem can be brought under control, before it gets out of hand [9].

Unfortunately, we still do not have either *in vivo* or *in vitro* model systems to study or to dissect the exact mechanism for NeuroAIDS, as well as to evaluate efficacy of drugs. Under these circumstances, the world community needs to pay more attention on research efforts by allocating funding to find the means either to control NeuroAIDS or at least to improve the health status of these patients. The menace of NeuroAIDS requires urgent and important attention before its control gets out of hand or drain lot of resources in an already depressed world economy.

ACKNOWLEDGEMENTS

Authors are thankful to Prof. S. M. P. Khurana, Director, AIB, Amity University Uttar Pradesh, NOIDA, India, for providing necessary resources and facilities for completion of this manuscript. Authors are also thankful to Mr. Dinesh Kumar for secretarial assistance.

REFERENCES

- [1] Prince M, Patel V, Saxena S, et al. [2007] No health without mental health. *Lancet* 370(9590): 859–877.
- [2] Power C, Boisse L, Rornke S, et al. [2009] NeuroAIDS: An evolving epidemic. *Can J Neurosci* 36: 285–95.
- [3] Gottlieb MS, Schroff R, Schanker HM, et al. [1981] Pneumocystis carinii pneumonia and mucosal candidiasis in previously healthy homosexual men: evidence of a new acquired cellular immunodeficiency. *N Engl J Med* 305: 1425–1431.
- [4] Verma AS, Bhatt SM, Singh A, Dwivedi PD. [2009] HIV: An Introduction. In: Varma A, Chauhan AK, editors. Text book on molecular biotechnology. Delhi: I.K. International Publishing House Pvt. Ltd., India, p. 853–878.
- [5] UNAIDS Report–2009.
- [6] Verma AS, Singh A, Singh UP, Dwivedi PD. [2010] NeuroAIDS in Indian Scenario. In: Gaur RK, Sharma P, et al, editors. Recent trends in biotechnology and microbiology. *Nova Science Publishers, Inc.*, New York, USA, p. 155–167.
- [7] Gonzalez-Scarano F, Martin-Garcia J. [2005] The neuropathogenesis of AIDS. *Nat Rev Immun* 5: 69–68.
- [8] Verma AS, Singh UP, Dwivedi PD, Singh A. [2010] Contribution of CNS cells in NeuroAIDS. *J Pharm Bioall Sci* 2: 300–306.
- [9] Ghafouri M, Amini S, Khalili K, et al. [2006] HIV-1 associated dementia: symptoms and causes. *Retrovirology* 3: 28.

ABOUT AUTHORS



Ashish S. Verma has completed his education from Gorakhpur University, Gorakhpur, India. His doctoral work is in the area of tumor immunotherapy and toxicology from Industrial Toxicology Research Center, Lucknow, India. After his PhD, he moved to USA and worked in the area of signal transduction and HIV. He has published more than 25 research papers in international journals. He has numbers of book chapters to his credit. He has published one book. At present, he is working as Professor of Biotechnology at Amity University Uttar Pradesh, NOIDA. He is also writing a couple of books on Biotechnology. His current area of research interest is NeuroAIDS and neuroinflammation.



Mr. Udai Pratap Singh has completed his M.Tech. degree in Biotechnology from Amity Institute of Biotechnology, Amity University Uttar Pradesh, NOIDA. Because of excellent credentials and reputation of being a studious and intelligent student of AIB, he has been appointed as Lecturer at AIB. In last one year he has published 1 research article, 2 popular articles and 2 book chapters. He has also published one book. Since he joined AIB, he became an active member of Prof. Verma's group and is actively pursuing his career in the area of NeuroAIDS and neuroinflammation.



Dr. Anchal Singh is presently working as Senior Lecturer, Amity Institute of Biotechnology, Amity University Uttar Pradesh, NOIDA. She has completed her doctoral studies at Department of Biochemistry, Banaras Hindu University, Varanasi. She has worked in the area of immunobiology and immunodiagnostic of filarial parasite. She has published 4 research publications in international journal, 3 book chapters. She has published one book and is currently writing two books. She has presented her work in various international and national meetings. At present she is a member of Prof. Verma's research group and working in the area of NeuroAIDS and neuroinflammation.

SCREENING AND CHARACTERIZATION OF STRESS TOLERANT SACCHAROMYCES CEREVISIAE ISOLATED FROM BREWERY EFFLUENTS FOR ANIMAL PROBIOTIC APPLICATIONS

Bhukya Bhima¹, Sudhakara Reddy Marrivada¹, Tangutur Anjana Devi³, Yerradoddi Ramana Reddy², and Linga Venkateswar Rao^{1*}

¹ Department of Microbiology, University College of Science, Osmania University, Hyderabad, AP– 500007, INDIA

² Department of Animal Nutrition, College of Veterinary Science, Sri Venkateshwara Veterinary University, Rajendranagar, Hyderabad, AP–500030, INDIA

³ Centre for chemical biology, Indian Institute of Chemical Technology, Uppal Road, Hyderabad, AP– 500007, INDIA

Received on: 4th-Aug-2010; Revised on: 10th-Nov-2010; Accepted on: 12th-Nov-2010; Published on: 10th-Dec-2010.

*Corresponding author: Email vrlinga@yahoo.com Tel: +91-40-27682246; Fax: +91-40-27090661

ABSTRACT

Based on the colony morphology and microscopic characteristics, 26 yeasts were isolated from different sources including brewery effluents. Initially they were screened for their thermotolerance at 40 °C and only 5 strains were selected. They were later grown in yeast extract peptone dextrose medium to screen their stress tolerance at five different temperatures; at different concentrations of a mixture of acetic, propionic and butyric acids; at different pH; at different concentrations of glucose and bile salts. Based on the growth at different stress conditions, yeast OBV9 was selected and characterized as Saccharomyces cerevisiae by sequencing its 5.8S rRNA gene and internal transcribed spacer (ITS) 1 and 2. The sequence obtained was most similar (99%) to S. cerevisiae, when it was blast searched in NCBI database and showed a separate branch in phylogenetic analysis.

Keywords: Probiotics yeast; characterization; stresstolerance; animals

[1] INTRODUCTION

Yeasts may be defined as microorganisms in which the unicellular form is conspicuous and which belong to fungi. No other group of microorganisms has been more intimately associated with the progress and well being of the human than yeasts [26]. The most commonly used probiotic yeast in animals is *Saccharomyces cerevisiae*. Yeasts of the genus *Saccharomyces* are usually revealed in sugar-rich natural substrates such as fruits and exudates of trees [20]. They have seldom been isolated from other habitats such as soils, plant leaves, and decaying plant debris [10]. Various yeast species found on grapes and on winery surfaces participate in spontaneous fermentations [25].

Yeast culture "*Saccharomyces cerevisiae*" is used in monogastrics and ruminants to stimulate and stabilize the processes that occur in the gastro-intestinal tract and help to increase competitive exclusion of undesired organisms in the

digestive tract thereby enhancing the performance of livestock [26]. The effects of yeast culture on animal productivity are strain-dependant. So, all yeast culture preparations are not equivalent in efficiency. This aspect opens a new field of research for new strains, each being more specialized in its use [6]. Many studies did not find any difference in supplementing yeast to ruminants for increased milk production [27] and dry matter intake [15]. Some of the reasons might be high temperature i.e. 39 °C [12], bile salt concentration, osmotic pressure and organic acids in the rumen [11, 16]. Normally, yeast *Saccharomyces cerevisiae* grows at mesophilic range of temperature (30°C) and pH. 4.5 - 5.5 [17]. Since the rumen environment is so diversified, some strains of this yeast may or may not tolerate and survive. Considering the above parameters, it is of importance to develop thermo, acid, bile and osmo tolerant yeast as probiotic. The present investigation was carried out to isolate, screen and characterize a new potential strain of yeast with the ability to tolerate diverse conditions of rumen.

[II] MATERIALS AND METHODS

2.1. Isolation of yeast

Sources selected for isolation of stress tolerant yeast were toddy [18] collected in hot summer, sugarcane juice [24], sugarcane bagasse [3], bakery wastes, molasses [5,19,2], nectar [4,13,20], soil samples from thermal power plant [14], fruits such as bananas, grapes, cherries [7,23] and brewery effluents. These sources are popularly known as good supporters and have intrinsic nutritional value for yeast growth. The source samples were serially diluted to ten fold in sterile distilled water and inoculated on yeast extract peptone dextrose agar (YEPDA, Yeast extract 1%, Peptone 1%, Dextrose 2% and Agar agar 2%) medium plates by spread plate method. These plates were incubated at 32 °C in incubator for 48 hours. After incubation developed colonies were observed for their morphology and microscopic characteristic. Isolated yeasts were preserved in YEPDA slants.

2.2. Preparation of inoculum

Equal amount of each of the yeast cultures from slants were inoculated into 250 ml conical flasks, each containing 100 ml YEPD broth medium and incubated at 32 °C and 150 rpm agitation in the shaker incubator for overnight. After incubation, culture medium was centrifuged at 5,000 rpm for 5 minutes. Pellet was washed with sterile distilled water twice and re-suspended in equal amount of sterile distilled water. This was freshly prepared each time and 1 per cent v/v was used as inoculum. After 48 hours incubation, culture broth was diluted several times to obtain proper optical density (OD<1.0). The OD of culture medium was measured at 660 nm in UV-Visible spectrophotometer (Pathlength-1.0 cm, Systronics 117) and it is represented by multiplying it with number of dilutions.

2.3. Screening for stress (thermo, acid, osmo and bile) tolerance

To detect the thermotolerance of isolated yeasts, each of the yeasts (total 26 yeasts) were inoculated onto the yeast extract peptone dextrose (YEPD) agar medium plates and incubated at 40 °C to test their thermotolerance. Based on the growth on the medium plates, yeast isolates were selected for further studies. To detect further temperature tolerance and growth at different temperatures, 5 selected yeasts were inoculated into 100 ml sterile YEPD broth medium flasks, incubated for 48 hours at 150 rpm and at 5 different temperatures 30, 35, 40, 42 and 44 °C in shaker incubator. After incubation, optical density (OD) was measured at 660 nm.

Simultaneously, to detect the acid tolerance, the yeast strains were inoculated into sterile YEPD broth medium with different concentrations of a mixture of organic acids [1] (acetate, propionate and butyrate, 70:20:10), 0.0, 0.25, 0.5 and 1.0 per cent, respectively. Flasks were incubated for 48 hours at 32 °C and 150 rpm in the shaker incubator. This was followed by measurement of OD of the culture at 660 nm. Similarly flasks, each containing 100 ml sterile medium with different pH values 2, 3, 4, 5, 6 and 7 were also inoculated with the same strains and incubated for 48 hours at 32 °C and 150 rpm agitation in the shaker incubator and OD₆₆₀ was measured.

The selected yeast strains were inoculated into sterile YEPD broth medium with 6 different concentrations of glucose 5, 10, 15, 20, 25 and 30 per cent, respectively. Flasks were incubated for 48 hours at 32 °C and 150 rpm agitation in the shaker incubator. After incubation, OD₆₆₀ was measured.

Each of the selected yeast strains were inoculated into sterile YEPD broth medium with five different concentrations 0.2, 0.4, 0.6, 0.8 and 1.0 per cent of bile salts (ox bile from Qualigens) [1]. Flasks were incubated

for 48 hours at 32 °C and 150 rpm agitation in the shaker incubator. After incubation, OD₆₆₀ was measured.

2.4. Characterization of yeast by rRNA gene sequencing

Selected stress tolerant yeast OBV9 was characterized by sequencing its 5.8S rRNA gene and internal transcribed spacer (ITS) 1 and 2 [21, 23] by *Macrogen Inc. Ltd.* (www.macrogen.com) using an automated DNA sequencer (model 3730XL12-20140-014). DNA extracted from the sample was further run in the gel electrophoresis and PCR was performed to amplify the 5.8S rRNA and internal transcribed spacer (ITS) 1 and 2 with forward and reverse universal primer pairs targeted to the 5.8S rRNA gene. The primers used in this study are universal primers ITS1 and ITS4 based on the conserved regions of 5.8S rRNA gene and ITS1 and ITS2 which is designed to detect wide range of yeast strains. Sequences of forward and reverse primers are 5'-TCCGTAGGTGAACCTGCGG-3' and 5'-TCCTCCGCTTATTGATATGC-3', respectively.

2.5. Analysis of sequence data and Nucleotide sequence accession number

Complete Sequence of 5.8S rRNA gene and partial sequences of internal transcribed spacer (ITS) 1 and 2 were blast searched in NCBI database (www.ncbi.nlm.nih.gov) for matching. Based on the BLAST results, phylogenetic and molecular evolutionary analyses were conducted using MEGA version 4 [30]. Species relationships were also investigated by using unweighted pair group with mathematical average (UPGMA) cluster analysis [28]. The 659 base pair length gene sequence which we determined in this study has been deposited in the NCBI-GENEBANK data library and acquired the accession number (GU229793).

2.6. Scanning electron microscopy (SEM) of *S. cerevisiae* OBV9

For SEM analysis, *S. cerevisiae* OBV9 cells were rinsed twice with sterile double-distilled water, and distributed on a 12 mm glass cover slip coated with poly-L-lysine (Sigma Diagnostics) then fixed for 50 min by incubating in a solution containing 2.5% glutaraldehyde in 0.1 M cacodylate buffer. The glass cover slip was washed twice in 0.1 M Sodium cacodylate buffer. To improve the surface architecture, fixed cells were rinsed thoroughly using 0.1 M cacodylate buffer, and treated with 6% thiocarbonylhydrazide. The glass cover slip was finally washed with double-distilled water and dehydrated through a graded series of ethanol solutions. It was then dried and sputter-coated (JEOL JFC-1600) with a gold layer and used for scanning.

2.7. Statistical analyses

The data obtained was analyzed statistically [29] and tested for significance by Duncan's multiple range test [8] was accepted at the level of (P<0.01).

[III] RESULTS

3.1. Isolation of yeast

Twenty six yeast strains were isolated from different sources (toddy, sugarcane bagasse, bakery oven wastes, molasses, soil samples from thermal power plant, nectar and samples of brewery effluents) based on their colony morphology and

microscopic observation. They were designated as OBV1, 2, 3, 4, 5, 6, 7, 8, 9, 10, 11, 12, 13, 14, 15, 16, 17, 18, 19, 20, 21, 22, 23, 24, 25 and 26. OBV1-6 were isolated from toddy, 7-9 from brewery effluents, 10-13 from bakery oven wastes, 14-19 from sugarcane bagasse, 20-22 from molasses, 23-24 from nectar and 25-26 from soil samples (thermal power plant). The

morphological features of yeast colony grown on YEPD agar for 48 hours were off white in colour, circular in shape, convex elevated with opaque opacity and smooth texture. Yeast cells were spherical and egg shaped with budding, when observed under microscope. The scanning electron microscopic picture of *Saccharomyces cerevisiae* OBV9 is shown in [Figure-1](#).

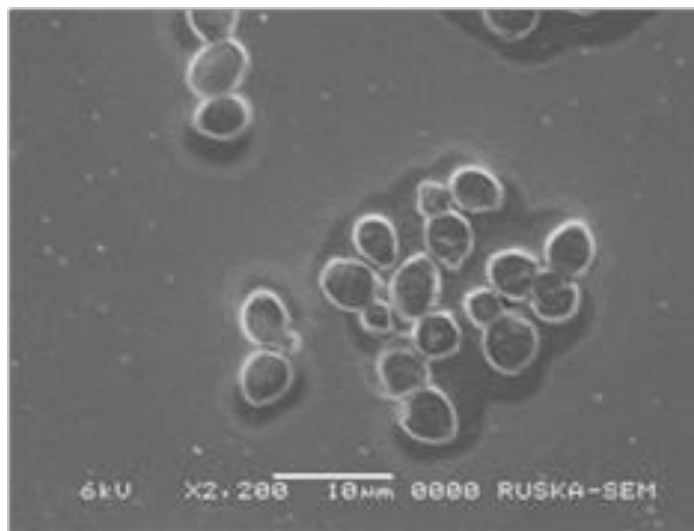


Fig: 1. Scanning electron micrograph of isolated yeast OBV9 showing budding cells under X2,200 magnification

3.2. Screening for stress tolerance and characterization

All the 26 strains were inoculated into yeast extract peptone dextrose (YEPD) agar medium plates and incubated at 40 °C to test their thermo tolerance. After 48 hours of incubation, plates were observed for growth and only 5 yeast strains were able to grow. These 5 strains (OBV4, OBV6, OBV9, OBV10 and OBV11) were later grown at five different temperatures 30, 35, 40, 42 and 44 °C.

To assess the ability of biomass production by yeasts at different temperatures, turbidity of the cultures was measured.

At 42 °C significant ($P < 0.01$) growth was observed for OBV9 and OBV11 [[Table- 1](#)].

The above five yeast strains were grown in YEPD medium with different concentrations (0.00, 0.25, 0.50 and 1.00 per cent) of a mixture (70:20:10) of acetic, propionic and butyric acids. After incubation, turbidity (OD_{660}) of the cultures was measured and found to be similar in 1 per cent organic acids medium for all the strains except OBV11 [[Table- 2](#)]. Similarly, all the 5 strains were grown in YEPD medium with different pH values 2, 3, 4, 5, 6 and 7 to screen acid tolerance. After incubation, turbidity was measured and at 2 pH, growth was found to be significant ($P < 0.01$) for OBV9 [[Table- 3](#)].

Table: 1. Effect of temperature on the growth of yeast

| Strain No. (OBV) | OD ₆₆₀ at temperature | | | | |
|---------------------|----------------------------------|-------|-------------------|-------------------|-------|
| | 30 °C | 35 °C | 40 °C | 42 °C | 44 °C |
| 4 | 6.34 | 6.41 | 3.99 ^a | 0.34 ^a | 0.33 |
| 6 | 5.97 | 6.51 | 4.24 ^a | 0.29 ^a | 0.24 |
| 9 | 6.38 | 6.49 | 5.15 ^b | 4.44 ^c | 0.34 |
| 10 | 6.26 | 6.41 | 3.88 ^a | 1.28 ^b | 0.25 |
| 11 | 6.42 | 6.48 | 5.73 ^c | 4.52 ^c | 0.31 |
| SEM | 0.11 | 0.07 | 0.20 | 0.52 | 0.02 |

Each value is an average of four observations

^{abc} values bearing different superscripts in a column differ significantly ($P < 0.01$). OD 1.0 = 2×10^6 yeast cells/ml

Table: 2. Effect of different concentrations of organic acids i.e. mixture of acetic, propionic and butyric acids (70:20:10) on the growth of yeast at 32 °C

| Strain No. (OBV) | OD ₆₆₀ at per cent organic acids | | | |
|---------------------|---|------|------|-------------------|
| | 0.0 | 0.25 | 0.50 | 1.00 |
| 4 | 6.34 ^b | 6.22 | 5.22 | 4.26 ^b |
| 6 | 6.12 ^b | 6.04 | 5.23 | 4.26 ^b |
| 9 | 6.45 ^b | 6.32 | 6.08 | 4.31 ^b |
| 10 | 4.26 ^a | 6.31 | 5.68 | 4.12 ^b |
| 11 | 6.36 ^b | 6.08 | 5.03 | 3.34 ^a |
| SEM | 0.22 | 0.17 | 0.13 | 0.12 |

Each value is an average of four observations

^{ab} values bearing different superscripts in a column differ significantly (P < 0.01)

Table: 3. Effect of pH on the growth of yeast at 32 °C

| Strain No. (OBV) | OD ₆₆₀ at pH | | | | | |
|---------------------|-------------------------|-------------------|-------------------|-------------------|------|-------------------|
| | 2.0 | 2.0 | 2.0 | 2.0 | 2.0 | 2.0 |
| 4 | 0.34 ^a | 2.68 ^b | 4.68 ^c | 6.34 ^d | 6.41 | 6.01 ^b |
| 6 | 0.27 ^a | 2.26 ^b | 4.24 ^b | 6.12 ^d | 6.01 | 5.97 ^b |
| 9 | 3.07 ^c | 5.33 ^d | 6.12 ^e | 6.45 ^b | 6.41 | 6.22 ^b |
| 10 | 0.28 ^a | 1.78 ^a | 3.88 ^a | 4.26 ^a | 6.11 | 5.34 ^a |
| 11 | 1.97 ^b | 4.66 ^c | 5.01 ^d | 6.36 ^b | 6.32 | 5.89 ^b |
| SEM | 0.31 | 0.37 | 0.21 | 0.22 | 0.19 | 0.17 |

Each value is an average of four observations

^{abcde} values bearing different superscripts in a column differ significantly (P < 0.01)

To determine osmo tolerance, all the 5 strains were grown in YEPD medium with 5, 10, 15, 20, 25 and 30 per cent glucose. After incubation, tolerance at 30 per cent glucose was detected in terms of OD for two strains OBV9 and OBV11, respectively [Table-4]. Five sets of YEPD medium flasks with different concentrations of bile salts (0.2, 0.4, 0.6, 0.8 and 1.0 per cent) were inoculated with all the above five yeast strains to

determine their bile tolerance. After incubation, turbidity (OD₆₆₀) of the cultures was measured. The significant (P < 0.01) growth at 1 per cent level of bile was observed for yeast strains OBV9 and OBV11 [Table-5]. Based on the growth at different temperatures, a different concentration of organic acids, sugars, pH and bile salts, yeast isolate OBV9, isolated from brewery effluents was selected as a potential probiotic and characterized.

Table: 4. Effect of glucose on the growth of yeast at 32 °C

| Strain No. (OBV) | OD ₆₆₀ at glucose concentration (per cent) | | | | | |
|---------------------|---|------|------|------|-------------------|--------------------|
| | 5 | 10 | 15 | 20 | 25 | 30 |
| 4 | 6.44 | 6.52 | 6.68 | 6.23 | 3.36 ^b | 2.04 ^b |
| 6 | 6.48 | 6.54 | 6.58 | 6.21 | 2.27 ^a | 1.57 ^a |
| 9 | 6.54 | 6.69 | 6.82 | 6.68 | 6.31 ^c | 4.12 ^c |
| 10 | 6.34 | 6.41 | 6.68 | 6.28 | 3.25 ^b | 1.85 ^{ab} |
| 11 | 6.42 | 6.48 | 6.52 | 6.66 | 6.34 ^c | 4.33 ^c |
| SEM | 0.05 | 0.05 | 0.04 | 0.07 | 0.48 | 0.33 |

Each value is an average of four observations

^{abc} values bearing different superscripts in a column differ significantly (P < 0.01)

Table: 5. Effect of bile salts (ox bile) on the growth of yeast at 32 °C

| Strain No. (OBV) | OD ₆₆₀ at ox bile conc. (per cent) | | | | |
|---------------------|---|------|-------------------|-------------------|-------------------|
| | 0.2 | 0.4 | 0.6 | 0.8 | 1.0 |
| 4 | 6.12 | 6.22 | 3.34 ^a | 1.83 ^a | 1.56 ^a |
| 6 | 6.07 | 6.11 | 4.02 ^b | 2.63 ^b | 1.38 ^a |
| 9 | 6.44 | 6.49 | 5.85 ^d | 4.78 ^c | 3.74 ^b |
| 10 | 6.22 | 6.04 | 3.91 ^b | 2.88 ^b | 1.51 ^a |
| 11 | 6.30 | 6.38 | 5.13 ^c | 4.66 ^c | 4.17 ^b |
| SEM | 0.06 | 0.07 | 0.26 | 0.31 | 0.33 |

Each value is an average of four observations
^{abcd} values bearing different superscripts in a column differ significantly (P< 0.01)

Characterization of stress tolerant yeast by 5.8S rRNA gene and ITS1 and ITS2 sequencing showed that it was most similar (99%) to *S.cerevisiae*. Nucleotide sequences were submitted to Gene Bank for accession number – [GU229793](#). The optimal tree with the sum of branch length = 0.00970218 is shown in [Figure-2](#). The percentage of replicate trees in which the associated taxa clustered together in the bootstrap test (500 replicates) is shown next to the branches [9]. The tree is drawn to scale, with branch lengths in the same units as those of the evolutionary distances used to infer the phylogenetic tree. The evolutionary distances were computed using the Maximum Composite Likelihood method [31] and are in the units of the

number of base substitutions per site. All positions containing gaps and missing data were eliminated from the dataset (Complete deletion option). There were a total of 659 positions in the final dataset. Yeast OBV9 has exhibited an individual sub line that displayed little phylogenetic affinity with other *Saccharomyces* species. Of the 17 *Saccharomyces* species and one uncultured fungal clone, 12 species of *Saccharomyces* showed a distinct group related to each other displaying levels of 5.8S rRNA gene and ITS1 and ITS2 sequence similarity of 99% and 3 showed distinct groups with 99% similarity. Based on this analysis, stress tolerant yeast isolate OBV9 was characterized as *Saccharomyces cerevisiae* OBV9.

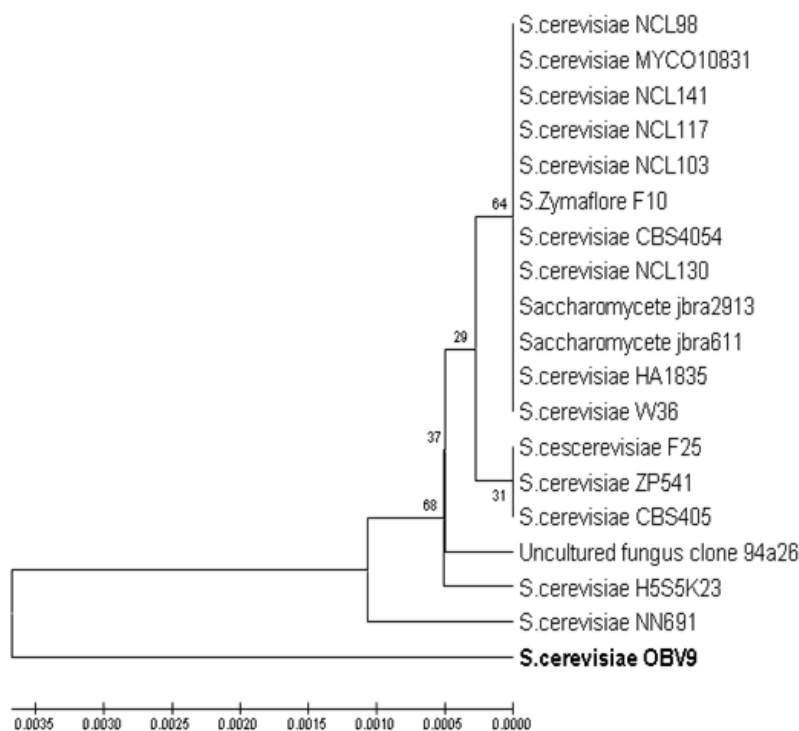


Fig: 2. Phylogenetic tree of *Saccharomyces cerevisiae* OBV-9 associated with other members of *Saccharomyces* genus. Distance matrix was calculated using UPGMA and topology was inferred by Neighbor-joining method based on the bootstrap analysis of 500 trees

[IV] DISCUSSION

Strains isolated from a particular region are usually more adapted to their own climatic conditions and therefore the isolation of such organism was obvious because these strains were isolated from high temperature environment (Bakery oven wastes and soil samples from thermal power plants) and high sugar concentration as observed in fruits, molasses, nectar etc. In the present study, Yeast Extract Peptone Dextrose (YEPD) medium [32] was used for the screening of yeast strains.

Though significant growth was obtained at 40 °C by OBV11, among all the strains OBV9 and OBV11 were able to produce significant ($P < 0.01$) biomass at 42 °C in terms of OD_{660} and therefore described as thermotolerant yeasts. This thermotolerance is in agreement with Preeyaporn *et al.* [22] where the authors isolated thermotolerant yeast which can tolerate 41 °C. At 44 °C there was no significant ($P > 0.01$) growth obtained for any of the yeast strains. Significant ($P < 0.01$) biomass in terms of OD was obtained by the strain OBV9 in the medium with pH 2. This might be due to its high acid tolerance. Significant lower biomass was observed for OBV11 compared to all other strains in the medium containing 1 per cent organic acids. The yeast strains OBV9 and OBV11 were able to produce significant ($P < 0.01$) biomass in the medium containing 25 per cent glucose. Significant ($P < 0.01$) biomass in 30 per cent glucose medium was also obtained by OBV9 and OBV11 compared to other strains. This might be due to their high osmo tolerance. The growth obtained by OBV6 and OBV10 was not significantly ($P > 0.01$) different from each other in 0.6 per cent bile salts medium. However, the significant ($P > 0.01$) growth in 0.6 per cent bile salts medium was obtained by the strain OBV-9. In the medium containing 0.8 per cent bile salts, significant ($P < 0.01$) growth was obtained by OBV9 and OBV11. Similarly, in 1 per cent bile salts medium also, significant ($P < 0.01$) growth was observed for OBV9 and OBV11. But it was not significantly ($P > 0.01$) different between both of the strains. Based on growth performance in all the above conditions OBV9, isolated from brewery effluents was selected and characterized. The gene sequence showed similarity of 99% with *Saccharomyces cerevisiae*, while the similarity was less with other organisms.

Alignment with corresponding sequences of the 17 other strains of *Saccharomyces* and one uncultured fungal clone was performed and a phylogenetic tree was constructed using the neighbor-joining method. The 5.8S rRNA gene and ITS1 and ITS2 based phylogenetic analysis revealed the presence of two branches. A first branch comprising the 9 strains of *Saccharomyces cerevisiae* 2 *Saccharomycetes* and one *Saccharomyces zymaflore* were appeared as a sister group while based on the sequence data and other molecular characters, yeast strain OBV9 appeared as a separate branch within the *Saccharomyces cerevisiae* strains. It is concluded that the stress

tolerant *Saccharomyces cerevisiae* OBV9 is a promising candidate for ruminant probiotic applications.

[V] CONCLUSION

Since the yeast *Saccharomyces cerevisiae* OBV9 tolerates temperature up to 44 °C, pH 2, sugar concentration up to 30 per cent and 1 per cent bile salt, it is described as a stress tolerant yeast. All these stress conditions prevail in gastro intestinal tract (rumen) of animals. Since it tolerates all the stress conditions present in gastro intestinal tract of animals, OBV9 is a promising candidate for ruminant probiotic applications.

FINANCIAL DISCLOSURE

This study has been supported by grants from the Department of Biotechnology (DBT), Ministry of Science and Technology, New Delhi, India.

ACKNOWLEDGEMENT

We thank our research scholars K. Chaitanya and Vijay Kumar, Department of Microbiology, Osmania University for their technical assistance.

REFERENCES

- [1] Agarwal N, Kamra DN, Chaudhary LC, Sahoo A, Pathak NN. [2000] Selection of *Saccharomyces cerevisiae* strains for use as a microbial feed additive. *Lett Appl Microbiol* 31: 270–273.
- [2] Ali D, Rabindra RJ, Ramanujam B, Rahimi M. [2008] Evaluation of different media and methods of cultivation on the production and viability of entomopathogenic fungi, *Verticillium lecanii* (Zimm.) viegas. *Pakistan J Biol Sci* 11: 1506–1509.
- [3] Amany HA, Neveen SG [2005] An enrichment of xylanolytic organism with high optima. *Biotechnol* 4: 49–55.
- [4] Carla CC Ruivo, Marc-Andre Lachance, Carlos A Rosa, Mauricio Bacci Jr, Fernando CP. [2006] *Candida heliconiae* sp. nov., *Candida pinguabensis* sp. nov. and *Candida saopaulonensis* sp. nov., three ascomycetous yeasts from *Heliconia veloziana* (Heliconiaceae). *International J Syst and Evol Microbiol* 56: 1099.
- [5] Chandrasena G, Keerthipala AP, Walker GM. [2006] Isolation and characterisation of Sri Lankan yeast germplasm and its evaluation for Alcohol Production. *J institute of brewing* 112: 302–307.
- [6] Denev SA, Peeva TZ, Radulova P, Stancheva N, Staykova G, Beev G, Todorova P, Tchobanova S. [2007] Yeast cultures in ruminant nutrition. *Bulg J Agric Sci* 13: 357–374.
- [7] Dilmani Warnasuriya, Liyanage AW, Weerawansa GG, Athauda PK, Jayatissa PM. [1985] Isolation and characterization of yeasts of some fruits and fruit products of Sri Lanka. *J National Sci Council* 13: 71–75.
- [8] Duncan DB. [1955] Multiple range and multiple 'F' test. *Biometrics* 11: 1–42.

- [9] Felsenstein J. [1985] Confidence limits on phylogenies: An approach using the bootstrap. *Evolution* 39: 783–791.
- [10] Glushakova AM, Yurkov AM, Chernov IY. [2007] Massive isolation of anamorphous ascomycete yeasts *Candida oleophila* from plant Phyllosphere. *Microbiol* 76: 799–803.
- [11] Jin LZ, Ho YW, Abdullah N, Jalaludin S. [1998] Acid and bile tolerance of *Lactobacillus* isolated from chicken intestine. *Lett Appl Microbiol* 27: 183–185.
- [12] Kamra DN. [2005] Rumen microbial ecosystem. *Current Sci* 89: 124–135.
- [13] Kathiresan K, Srinivasan K. [2005] Making artificial honey using yeast cells from salivary glands of honey bees. *Indian J Expt Bot* 43: 664–666.
- [14] Kiran Sree N, Sridhar M, Suresh K, Banat IM, Venkateswar Rao L. [2000] Isolation of thermotolerant, osmotolerant, flocculating *Saccharomyces cerevisiae* for ethanol production. *Bioresource Tech* 72: 43–46.
- [15] Kung L, Muck RE. [1997] Animal response to silage additives. In: Proceedings of the conference on Silage: Field to feed bunk. *North American Conference Hershey*. pp. 200–210.
- [16] Lankaputhra WEV, Shah NP. [1995] Survival of *Lactobacillus acidophilus* and *Bifidobacterium* species in the presence of acid and bile salts. *Cultured Dairy Prod J* 30: 113–118.
- [17] Lopez J. [2000] Probiotics in animal nutrition. *Asian Australian J Anim Sci* 13: 12–26.
- [18] Majeed Ahmad, Razzaque Chaudhury A, Ahmad KU. [1954] Studies on Toddy Yeast. *Mycological Society of America*. 708.
- [19] Marcia Luciana Cazetta, Maria Antonia and Celligoi, PC. [2006] Study of molasses/vinasse waste ratio for single cell protein and total lipids production. *Semina: Ciências Exatas Tecnológicas, Londrina* 27: 03–10.
- [20] Muhammad Mushtaq, Sharfun-Nahar, Hashmi MH. [2004] Isolation and identification of yeast flora from soil of Karachi, Pakistan. *Pakistan J Bot* 36: 173–180.
- [21] Pasha C, Kuhad RC, Venkateswar Rao L. [2007] Strain improvement of thermotolerant *Saccharomyces cerevisiae* VS3 strain for better utilization of lignocellulosic substrates. *J Appl Microbiol* 103: 1480–1489.
- [22] Koritha P, Dubois E, Scherens B, Jacobs E, Boonchirda C, Messenguyb F. [2008] Identification and characterization of a thermotolerant yeast strain isolated from banana leaves. *Sci Asia* 34: 147–152.
- [23] Rao RS, Bhadra B, Shivaji S. [2008] Isolation and characterization of ethanol producing yeasts from fruits and tree barks. *Lett Appl Microbiol* 47: 19–24.
- [24] Ravi Kumar M, Adharvana chary M, Lakshmi Narasu M. [2007] Isolation of novel strains from natural sources for biotransformation studies. *Res J Microbiol* 2: 94–97.
- [25] Redzepovic S, Orlic S, Sikora S, Majdak A, Pretorius IS. [2002] Identification and characterization of *Saccharomyces cerevisiae* and *Saccharomyces paradoxus* strains isolated from Croatian vineyards. *Lett Appl Microbiol* 35: 305–310.
- [26] Rita Sherma, Nangia OP, Gupta M, Sharma R. [1998] Effect of yeast culture (*Saccharomyces cerevisiae*) plus growth medium supplementation on rumen fermentation in buffalo calves fed high roughage diet. *International J Anim Sci* 13: 121–126.
- [27] Salama AAK, Caja G, Garin D, Albanell E, Such X, Casals R. [2002] Effects of adding a mixture of malate and yeast culture (*Saccharomyces cerevisiae*) on milk production of Murciano-Granadina dairy goats. *Anim Res* 51: 295–303.
- [28] Sneath PHA, Sokal RR. [1973] Numerical Taxonomy. Freeman, San Francisco. 573.
- [29] Snedecor GW, Cochran WG. [1980] Statistical methods. 7th edition. *The Iowa State University Press*. Iowa, USA.
- [30] Tamura K, Dudley J, Nei M, Kumar S. [2007] MEGA4: Molecular Evolutionary Genetics Analysis (MEGA) software version 4.0. *Molecular Biology and Evolution* 24: 1596–1599.
- [31] Tamura K, Nei M, Kumar S. [2004] Prospects for inferring very large phylogenies by using the neighbor-joining method. In: *Proceedings of the National Academy of Sciences* 101: 11030–11035.
- [32] Thais M, Guimaraes, Danilo G, Moriel, Iara P, et al. [2006] Isolation and characterization of *Saccharomyces cerevisiae* strains of winery interest. *Brazilian J Pharma Sci* 42: 119–126.

ABOUT AUTHORS



Linga Venkateswar Rao; MSc, PhD, is Professor and Chairman, Board of studies in Microbiology, Osmania University, Hyderabad having 30 years of teaching and research experience mainly in the area of Industrial Microbiology and Microbial Biotechnology. The research interests include understanding the thermotolerance mechanism of yeast strains, production of biofuel from lignocellulosic substrates, Probiotics for both human and animal applications. Produced 16 PhDs and at present 12 students are working under his supervision. He has been elected as a fellow of Biotech research society of India in 2004 and also elected as fellow of Andhra Pradesh Academy of Sciences in 2006. Visited USA (1999) to present a paper at Centenary Meeting of American Society for Microbiology held at Chicago. Published about 60 papers and presented nearly 100 papers in various conferences.



Bhukya. Bhima; M.Sc., Ph.D., is Assistant professor of Microbiology has 6 years of teaching and 10 years of research experience mainly in the area of Food and Environmental Microbiology. His research interests include development of stress tolerant probiotic organisms for animal feed supplementation. Published 8 papers, 1 book chapter and presented more than 30 papers in various national and international conferences. Visited South Korea in 2007 for attending the HUPO 6th annual world congress. Awarded AOHUPO/KSMS young scientist award 2007 by Human Proteome Organization at Seoul, South Korea during the 6th HUPO annual world congress 2007.



Sudhakara Reddy Marrivada, M.Sc., (Ph.D.), is Research Scholar of Microbiology has 5 years of research experience mainly in the area of probiotics. His research interests include development of stress tolerant probiotic organisms for animal feed supplementation. Published 3 papers, 1 book chapter and presented more than 10 papers in various national and international conferences.



Tangutur. Anjana Devi, M.Sc., Ph.D., is a Scientist in the Chemical Biology Division of the Indian Institute of Chemical Technology (IICT) has 10 years of research experience mainly in the area of Plant Proteomics and Molecular biology. Her research interests include Understanding the Proteome of various plants involved in different stress conditions. Published 3 original research papers and presented more than 5 papers in various national and international conferences.



Yarradoddi. Ramana Reddy, M.V.Sc., Ph.D., is Associate professor of Animal Nutrition in the Department of Animal Nutrition, College of Veterinary Science, has 9 years of teaching and research experience mainly in the area of Probiotics and Animal Nutrition. His research interests include supplementation of probiotic organisms for enhanced feed utilization in Meat and Milch animals. Published 20 papers, 1 book chapter and presented more than 50 papers in various national and international conferences.